博　　士　　論　　文

Effects of Initial Texture on Development of
Heterogeneous-nano Structure in a Cu-Zn System Alloy

金沢大学大学院自然科学研究科
機械科学専攻

学 籍 番 号　2124032009
氏　　名　李 研碩
主任指導教員　渡邊 千尋
提 出 年 月　令和 6 年 1 月 9 日

Doctoral Dissertation

Effects of Initial Texture on Development of Heterogeneous-nano Structure in a Cu-Zn System Alloy

Division of Mechanical Science and Engineering

Graduate School of Natural Sciences and Technology

Kanazawa University

Yanshuo Li

Jan. 2024

Contents

Chapter I General introduction

Copper alloys are extensively used in mechanical manufacturing and electrical engineering because of their favorable electrical conductivity and mechanical properties. Due to the rapid development and widespread use of the “Internet of Things” in home appliances and electric vehicles, the demand for miniaturized and lightweight electronic devices has increased. The development of high-strength copper alloys is essential to meet this demand.

Grain refinement is a method used to increase the strength of metallic materials. Severe plastic deformation (SPD) method is a representative technique used for grain refinement. In recent years, SPD processing has been applied to copper alloys to achieve ultrafine-grained (UFGed) microstructures and enhance strength without deteriorating electrical conductivity. Typical SPD methods include equal-channel angular pressing (ECAP) [1.1], high-pressure torsion (HPT) [1.2], multi-directional forging (MDF) [1.3], and accumulative roll bonding (ARB) [1.4], etc. As shown in Table 1.1, the SPD processes can result in UFGed structures of copper alloys and are an effective technique for enhancing their mechanical properties. However, almost all SPD processes invented to date are batch processes based on “shape-invariant deformations,” which have a strong limitation of applicable sample size. The tiny size applicable results in the inability to fabricate much larger products in practical demand and leads to high manufacturing costs. Therefore, the application of SPD methods in actual industrial production is currently quite rare.

Recently, Miura *et al.* first showed that a simple and heavily cold-rolled Cu-Zn alloy achieved extremely high mechanical properties comparable to or superior to those of the UFGed Cu-Zn alloy processed by MDF [1.5]. These excellent mechanical properties are attributed to the formation of a complex heterogeneous-nano (HN) structure composed of deformation-induced structures such as deformation twin domains, shear bands, and low-angle lamellae. The HN structure has been reported to develop in many FCC metals and alloys with low stacking fault energy (SFE), such as Cu-Be alloys, Cu-Ti-Co alloys, and SUS316LN austenitic stainless steels that were processed by simple and heavy cold rolling [1.6-1.8]. Improvements in mechanical properties by the application of the HN structure can be attained without significant changes to the existing manufacturing process, and thus can be easily applied to actual industrial mass production. Therefore, the application of HN structure to improve the strength of metallic materials has attracted much attention as a new microstructure control technique.

By combining the strengthening of the HN structure in the matrix with precipitation strengthening, the strength can be further improved without losing the electrical conductivity of the precipitation-strengthened copper alloy. The HN-structured Cu-1.86Be-0.23Co (mass%) alloy simultaneously achieves a high tensile strength (1.78GPa and electrical conductivity (21.8% IACS) comparable to conventional alloys [1.9]. The development of the HN structure was also confirmed in the heavy cold-rolled Cu-2.3mass% Ti alloy, and a tensile strength of 1.1 GPa and conductivity of 23% IACS were achieved [1.10]. After the aging treatment, the Cu-4.2Ni-0.93Si (mass%) alloy containing

the HN structure exhibited a tensile strength of 1061MPa and conductivity of 33% IACS [1.11]. Due to the low thermal stability of the HN structure [1.12], these precipitation-strengthened copper alloys tend to recrystallize before the elements in the matrix are fully precipitated. Therefore, it is necessary to explore aging conditions that can be applied to HN-structured materials without recrystallization. Miura *et al.* recently found that the addition of a small amount of argentum (Ag) to Cu-Zn system alloys can significantly improve their thermal stability [1.13, 1.14]. The Cu-Zn-Ag alloys exhibit grain boundary segregation of Ag, resulting in further improvements in both thermal stability and electrical conductivity [1.14]. In conclusion, HN-structured copper alloys superimpose multiple strengthening mechanisms of grain refinement strengthening, work hardening, precipitation strengthening, and grain boundary segregation strengthening by adjusting the aging conditions and chemical composition to ultimately achieve both high strength and conductivity.

Watanabe *et al.* recently investigated the evolution of HN structure in detail using SUS316LN austenitic steel [1.15]. They showed that mechanical twinning occurred in the existing coarse grains in the early stage of rolling, and that the twinned grains were subdivided by shear banding to form twin domains on subsequent rolling. Eventually, the HN structure was fully developed [1.15]. Aoyagi *et al.* investigated the deformation behavior of HN-structured materials by means of multiscale crystal plasticity simulation and showed that the tensile strength of the HN-structured material increases with an increase in the volume fraction of the twin domains in HN structures [1.16]. Therefore, it can be considered that mechanical twinning at the early stage of rolling strongly affects the volume fraction of twin domains in the finally developed HN structure, which consequently affects the mechanical properties of the HN-structured materials.

Currently, microstructure control of the HN structure is mainly accomplished by the addition of alloying elements. A reduction in the SFE of the alloy caused by the addition of elements can promote mechanical twinning. Miura *et al.* investigated the impact of Be content on the development of the HN structure in Cu-Be alloys [1.17]. As the Be content in the Cu-Be alloy increases from 0.4 to 2.14 mass%, the SFE decreased from 42 mJ/m^2 to 5 mJ/m^2 and the volume fraction of the twin domains in the 90% cold-rolled samples increased from almost 0% to 4.9% [1.17]. Moreover, increasing deformation resistance is also a way to promote mechanical twinning [1.18]. Matsuura *et al.* applied pre-aging to a high-concentration Corson alloy before rolling to increase its deformation resistance through precipitation hardening [1.11]. After 90% rolling, the volume fraction of the twin domains for the sample without pre-aging was 7%, whereas for the sample after pre-aging, it was 15% [1.11]. The essence of the above methods for controlling the HN structure is mechanical twinning in the early stages of rolling. In addition to factors such as the SFE and deformation resistance, the external stress state and crystallographic orientation of grains are also important factors that cannot be ignored in mechanical twinning.

The literature above demonstrates that mechanical twinning occurring during the early stage of rolling significantly affects the volume fraction of twin domains in the eventually developed HN structure. Although previous studies clearly demonstrated the effects of

addition elements on the evolution of the HN structure, the role of the crystallographic orientation on mechanical twinning during the development of the HN structure has not been clarified yet. Hence, the present dissertation investigates the impacts of different cold-rolling processes and different initial textures on the development of the HN structure, and their mechanical properties were investigated using a Cu-Zn system alloy.

This dissertation consists of the following chapters.

Chapter I General introduction

Chapter II Effects of rolling processes on the development of heterogeneous-nano structure and mechanical properties in a Cu-Zn system alloy

In Chapter II, the effects of the rolling processes on the development of the HN structure and mechanical properties of a Cu-38mass%Zn alloy were investigated. Rectangular-shaped specimens were subjected to two different rolling processes at room temperature. One was conventional unidirectional rolling (1DR) up to maximum thickness reduction of 90%. The other was rotational rolling (RR), in which the rolled surface rotated 90° around the rolling direction during the early stages of cold rolling (0~50%) and subsequently unidirectionally rolled up to a total reduction of 90%. For a total reduction of 50%, the number of grains with deformation twins in the RR specimens were higher than that in the 1DR specimen. Further cold rolling up to 90% produced HN structure in the specimens. The twin domains in the RR specimens were finer, and their volume fraction was larger than those in the 1DR specimen. In addition, the RR specimens exhibited better strength-elongation balances than the 1-DR specimen. It can be concluded that a larger volume fraction of the twin domains effectively improved the strength-elongation balance in the RR specimens.

Chapter III Effects of initial orientation in normal direction on the development of heterogeneous-nano structure and mechanical properties in a Cu-Zn system alloy

The experimental results in Chapter II strongly suggest that the initial texture in the normal plane is essential for mechanical twinning during the early stage of cold rolling. The effects of orientation in the normal direction (ND) on the formation of deformation twins in the early stage of cold rolling were discussed in Chapter III. Two Cu-38mass%Zn alloy specimens with different initial textures were used in this study. One had a strong <001> texture along the ND, and the other had a <111> texture. At the early stage of rolling, mechanical twinning occurred more frequently in the <001> specimen than in the <111> specimen. The difference in the twinning frequency can be reasonably explained by the difference in the ratio of the Schmid factor for twinning partial to that for perfect dislocation, and the <001> specimen had a significantly larger ratio than the <111> specimen. After 90% rolling, the <001> specimen exhibited a better strength-ductility balance than that of the <111> specimen because the <001> specimen had a higher volume fraction of deformation twin domains. It can be concluded that the initial texture

in the ND of the specimen plays an important role in the mechanical properties of the HN-structured materials via the formation of twin domains.

Chapter IV Effects of initial orientation in rolling direction on the mechanical twinning in a Cu-Zn system alloy

The influence of the orientation in the normal direction (ND) on mechanical twinning has been discussed in Chapter III. However, the crystal orientation parallel to the rolling direction (RD) should also affect twinning, as well as the orientation along the ND. The dependence of mechanical twinning on crystallographic orientation at the early stage of rolling was investigated in Chapter IV. For this purpose, the Cu-Zn-Sn alloy plate with a sharp <001> texture along the rolling plane (ND // <001>) was prepared, and the twinning behavior during rolling was studied in grains with three different orientations along the rolling direction (RD), that is, the rolling direction was parallel to <100>, <210>, and <110>. Precise examination revealed that grains with an RD // <110> orientation were most prone to twinning among the three. The effects of HN structure development on the tensile properties were systematically investigated. As the rolling reduction increased from 50% to 70%, the tensile strength increased significantly and the elongation to failure simultaneously increased. Considering the microstructural changes, the increase in the strength/ductility balance was attributed to the formation of the HN structure. Further rolling up to 90% resulted in a slight increase in the strength and a significant decrease in the ductility to approximately half of the value at 70%. It was suggested that the decrease in the volume fraction of twin domains in the HN structure, instead of an increase in the rolling texture components, during the rolling reduction from 70% to 90% complicatedly spoiled the strength-ductility balance.

Chapter V Summaries and prospects

This chapter summarizes the main results of this dissertation and provides prospects for studies on the orientation dependence of HN-structured materials.

Table 1.1 The grain size and strength of Cu alloys processed by SPD methods.

SPD method	Material	Grain size [nm]	Tensile stress [MPa]
ECAP	Cu-8 wt.% Ag [1.1]	109	720
HPT	Cu-2.5Ni-0.55Si (mass%) [1.2]	70	970
MDF	Cu-30mass%Zn [1.3]	20	970
ARB	Pure copper [1.4]	100	470

Reference

[1.1] Y.Z. Tian, S.D. Wu, Z.F. Zhang, R.B. Figueiredo, N. Gao and T.G. Langdon: Mater. Sci. Eng., A, 2011, 528(13-14), 4331-4336.

[1.2] H. Watanabe, T. Kunimine, C. Watanabe, R. Monzen and Y. Todaka: Mater. Sci. Eng., A, 2018, 730, 10-15.

[1.3] H. Miura, Y. Nakao and T. Sakai: Mater. Trans., 2007, 48(9), 2539-2541.

[1.4] A.R. Eivani, A. Shojaei, M.T. Salehi, H.R. Jafarian and N. Park: J. Mater. Res. Technol., 2021, 10, 291-305.

[1.5] H. Miura, Y. Takahashi, H. Yamaguchi and K. Kamibayashi: J. Japan Inst. Copper, 2010, 49(1), 51-55.

[1.6] H. Miura and R. Morita: J. Japan Inst. Copper, 2013, 52(1), 121-125.

[1.7] H. Miura, M. Kobayashi, I. Maki, H. Mori and Y. Ito: J. Japan Inst. Copper, 2016, 55(1), 190-196.

[1.8] H. Miura, M. Kobayashi, Y. Todaka, C. Watanabe, Y. Aoyagi, N. Sugiura and N. Yoshinaga: Scr. Mater., 2017, 133, 33-36.

[1.9] N. Muramatsu, H. Miura and C. Watanabe: J. Japan Inst. Copper, 2020, 59(1), 243-248.

[1.10] H. Miura, M. Kobayashi, Y. Ito, K. Maki, H. Mori and Y. Nakazato: J. Japan Inst. Copper, 2015, 54(1), 15-20.

[1.11] Y. Matsuura, H. Sakai, C. Watanabe, Y. Sumino and H. Miura: Mater. Trans., 2022, 63(4), 508-512.

[1.12] H. Miura, M. Kobayashi, T. Tsuji, T. Osuki, T. Hara and N. Yoshinaga: Mater. Trans., 2022, 63(3), 402-405.

[1.13] H. Miura, M. Kobayashi, Y. Ito, H. Mori and K. Maki: J. Japan Inst. Copper, 2021, 60(1), 67-73.

[1.14] H. Miura, K. Arai, M. Kobayashi, Y. Sumino and C. Watanabe: Mater. Trans., 2023, 64(5), 967-973.

[1.15] C. Watanabe, S. Kobayashi, Y. Aoyagi, Y. Todaka, M. Kobayashi, N. Sugiura, N. Yoshinaga and H. Miura: ISIJ Int., 2020, 60(3), 582-589.

[1.16] Y. Aoyagi, C. Watanabe, M. Kobayashi, Y. Todaka and H. Miura: Tetsu-to-Hagane, 2019, 105(2), 140-149.

[1.17] H. Miura, Y. Chiba, M. Kobayashi, C. Watanabe and N. Muramatsu: Mater. Trans., 2022, 63(10), 1431-1436.

[1.18] N. Narita and J. Takamura: F.R.N Nabarro (Ed.), Dislocations in Solids, 1992, 9(9), 135-189.

Chapter II Effects of rolling processes on the development of heterogeneous-nano structure and mechanical properties in a Cu-Zn system alloy

2.1 Introduction

As mentioned in Chapter I, compared to SPD processing, simple heavy cold rolling is easier to implement in industrial production, which can achieve high strength by introducing the HN structure. In particular, the volume fraction of the twin domains in the HN structure plays an important role in improving strength [2.1]. Research on the evolution of the HN structure indicated that the twin domains in the HN structure developed from twinned coarse grains [2.2]. Therefore, mechanical twinning occurred during the early stage of rolling should significantly affect the volume fraction of twin domains that eventually develop.

Mechanical twinning in coarse grains strongly depends on their crystallographic orientation with respect to the loading direction. Yang *et al.* subjected a Fe-33%Mn-2.93%Al-3%Si (mass%) alloy to tensile deformation and found that numerous deformation twins were formed in the grains with the <111> direction nearly parallel to the tensile direction [2.3]. Using the same alloy as Yang *et al.*, Meng *et al.* investigated the stress-axis dependence of the twinning behavior during compressive tests. They showed that deformation twins were preferentially formed in grains with the <001> direction nearly parallel to the compression axis [2.4]. These studies strongly suggest that the crystallographic orientations of the starting materials, that is, the initial texture, play a vital role in the formation of twins in polycrystalline materials during the cold-rolling process.

In Chapter 2, different cold-rolling processes are applied to a Cu-Zn system alloy. The effects of different processes on mechanical twinning during the early stages of rolling were systematically investigated. Additionally, the impacts of different cold-rolling processes on the development of the HN structure and their mechanical properties are discussed.

2.2 Experimental procedure

2.2.1 Rolling process

Commercial hot-extruded bars of Cu-37.75mass%Zn-0.11mass%Sn alloy were employed, and the chemical compassion of the alloy is listed in Table 2.1. Rectangular-shaped specimens were cut from the bars by a wire electric-discharge machine and subjected to cold rolling by two different processes. One is conventional unidirectional rolling (1DR) up to a maximum thickness reduction of 90% at room temperature. A schematic diagram of the other processes is shown in Fig. 2.1. The specimen was unidirectionally rolled up to 25% thickness reduction, the rolled surface was rotated 90° around the rolling direction, and rolling was continued up to a total reduction of 90%. This process of rotating once during the early stages of cold rolling (0~50%) is defined as one rotational rolling (1RR). In order to increase the number of rotations in the early stage of rolling, the rolled surface was rotated 90° around the rolling direction after every 12.5% reduction until the thickness was reduced to 50%. That is, the process in which the early stage of rolling was rotated three times, continuing rolling to a 90% reduction, was defined as 3RR. The rolling direction (RD), transverse direction (TD), and normal direction (ND) of the rolled sheet were determined from the final rolling pass.

2.2.2 Texture measurement

The textures of the specimens before and after rolling were measured by X-ray diffraction (XRD) from the ND plane using a Rigaku RINT2500. The specimens for the XRD analyses were ground down to half in thickness followed by polishing using a colloidal silica suspension and then, the X-ray beam was incident on the mirror-like plane. Texture measurements were performed using a Cu tube target (Cu-Kα, wavelength = 0.154 nm [2.5]) operating at 40 kV and 100 mA. The recalculated pole figures (RPFs), inverse pole figures (IPFs) and crystal orientation distribution functions (ODFs) were obtained using an analysis software (LaboTex®).

2.2.3 Microstructural observation

Microstructural observations were performed using field-emission scanning electron microscopy (FE-SEM; JEOL, JSM-7900F). Observations were mainly conducted on the TD plane at the center of the sheet thickness. The specimens for FE-SEM observation were mechanically polished using SiC papers (#2000) and then, electronically polished for approximately 100 s at 8 V and 233 K using a 30% nital solution (methanol : nitric acid = 7 : 3, volume ratio). The crystallographic orientations were analyzed using an electron backscattered diffraction (EBSD; OXFORD) camera equipped with an FE-SEM. The acceleration voltage and data acquisition interval (steps) for EBSD measurements were 20 kV and 50 nm, respectively.

2.2.4 Tensile test

Tensile tests were performed at room temperature at an initial strain rate of $\dot{\varepsilon} = 10^{-3}\ \mathrm{s}^{-1}$. As shown in Fig. 2.2, dog-bone-shaped specimens with a gauge dimension of

$5^L \times 2^W \times 1^T$ mm^3 were cut using an electric discharge machine so that the loading axis was parallel to the RD of the rolled specimens. The dog-bone-shaped specimens were mechanically polished using SiC papers (#2000) before the tensile tests.

Table 2.1 Chemical compassion of Cu-Zn alloy used in this study (mass%).

Cu	Zn	Sn	Pb
62.13	37.75	0.11	0.007

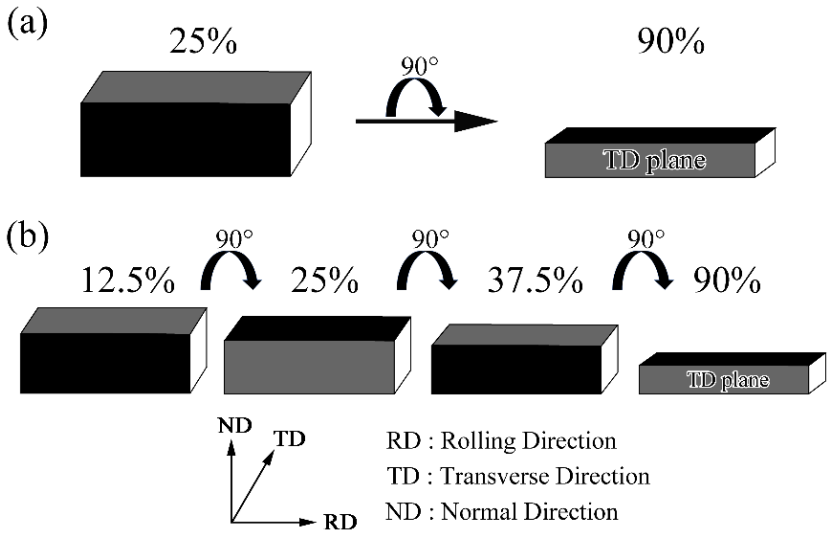

Fig. 2.1 Schematic diagrams of rotational rolling: (a) 1RR and (b) 3RR. The directions of the rolled sheets were determined by the final rolling pass.

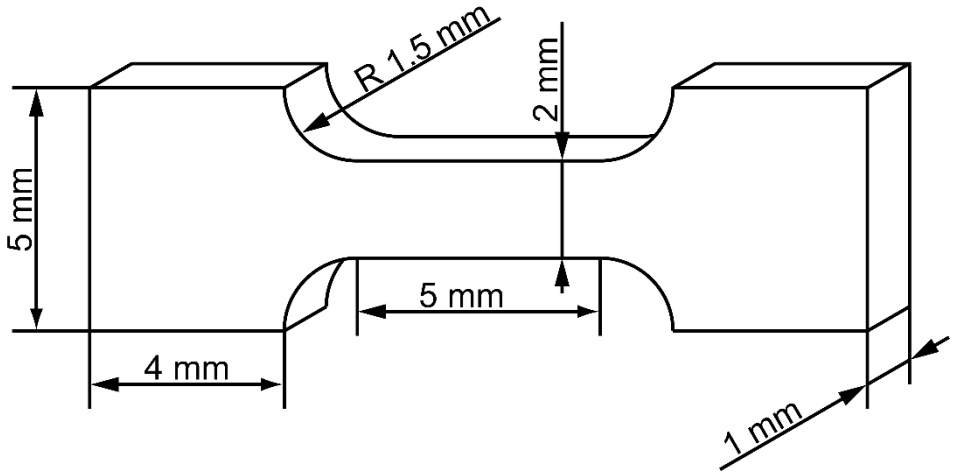

Fig. 2.2 Schematic illustration and dimensions of the specimens used for tensile tests.

2.3 Results

2.3.1 Initial microstructure and texture

Fig. 2.3 (a) shows a backscattered electron (BSE) image of the specimen before rolling. The initial grains before rolling exhibited nearly equiaxed shapes and someone contained annealing twins. As shown in Fig. 2.3 (b) and (c), SEM-EBSD analysis revealed that the <110> and <100> orientations were the main orientations of the ND plane, whereas the TD plane exhibited strong accumulation of the <100> orientation. As shown in Fig. 2.4, the global texture of the specimen was measured using XRD from the ND plane. Similar to the SEM-EBSD results, the orientations of the ND and TD planes exhibit large differences. In other words, the orientation of the rolled surface changed significantly during rotational rolling.

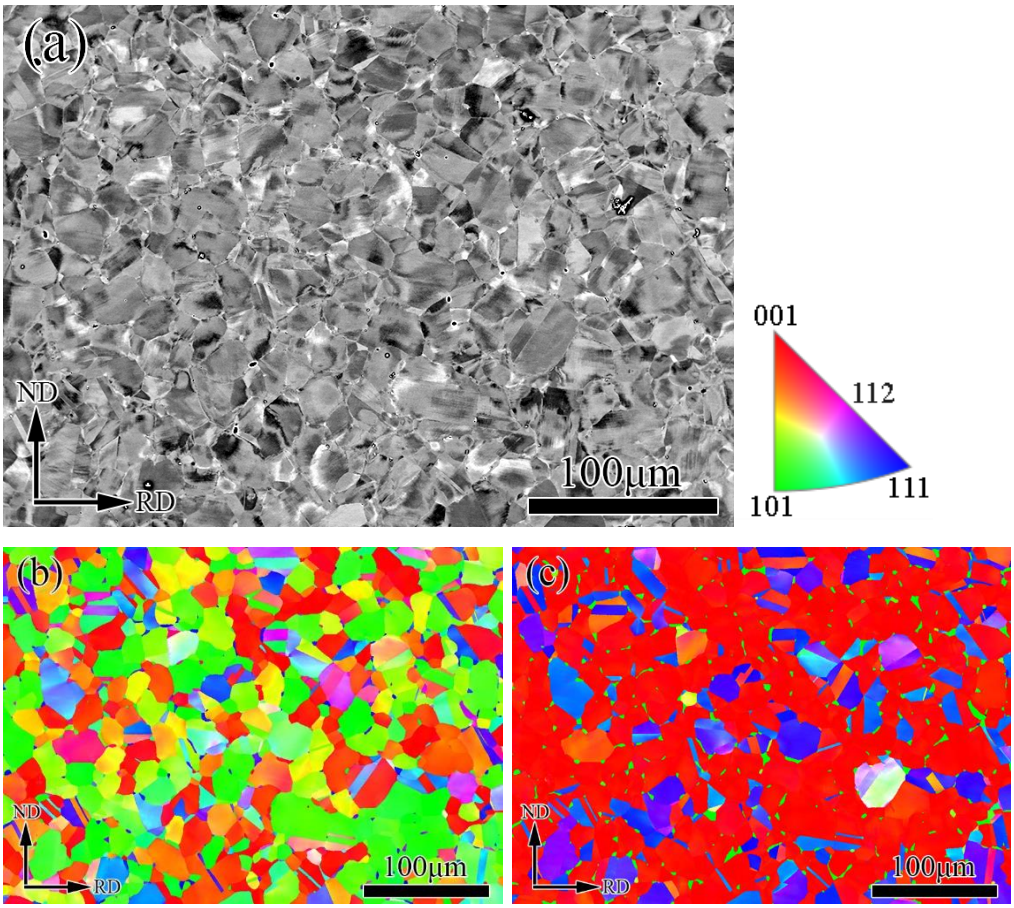

Fig. 2.3 (a) SEM-BSE image of specimen before rolling. (b) and (c) Inverse pole figure maps taken in the same area as in (a). Color decoding is parallel to (b) ND and (c) TD.

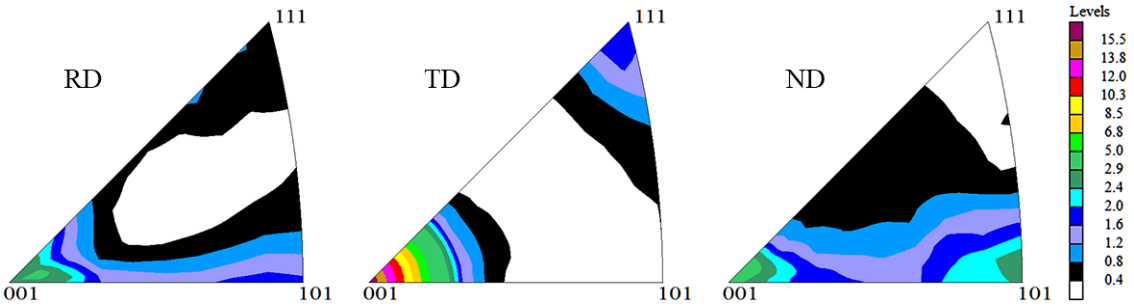

Fig. 2.4 Inverse pole figures of the specimen before rolling.

2.3.2 Deformation structure in the intermediate stage of rolling

Fig. 2.5 shows the band contrast maps observed from the TD of the 1DR, 1RR and 3RR specimens cold rolled to a 50% reduction. Twin boundaries (Σ3 grain boundaries) are indicated by red lines. Deformation twins were observed in all the specimens. The ratio of twinned grains to all grains (defined as the twin fraction) in several SEM images was calculated. The twin fractions for the 1DR, 1RR, and 3RR specimens were 51%, 76% and 81%, respectively. The rotational rolling process promotes mechanical twinning during the early stage of cold rolling. An increase in the number of rotations led to an increase in twin fraction. Not all twins could be detected in the present analyses because of the fine size of the twins and the crystallographic rotation within a grain caused by large plastic deformation. Therefore, twin fractions should be underestimated. However, because EBSD analyses were conducted under identical conditions (acceleration voltage, beam step, etc.) for all specimens, it can be stated that the twin fraction of the rotationally rolled specimen was larger than that of the unidirectionally rolled specimen.

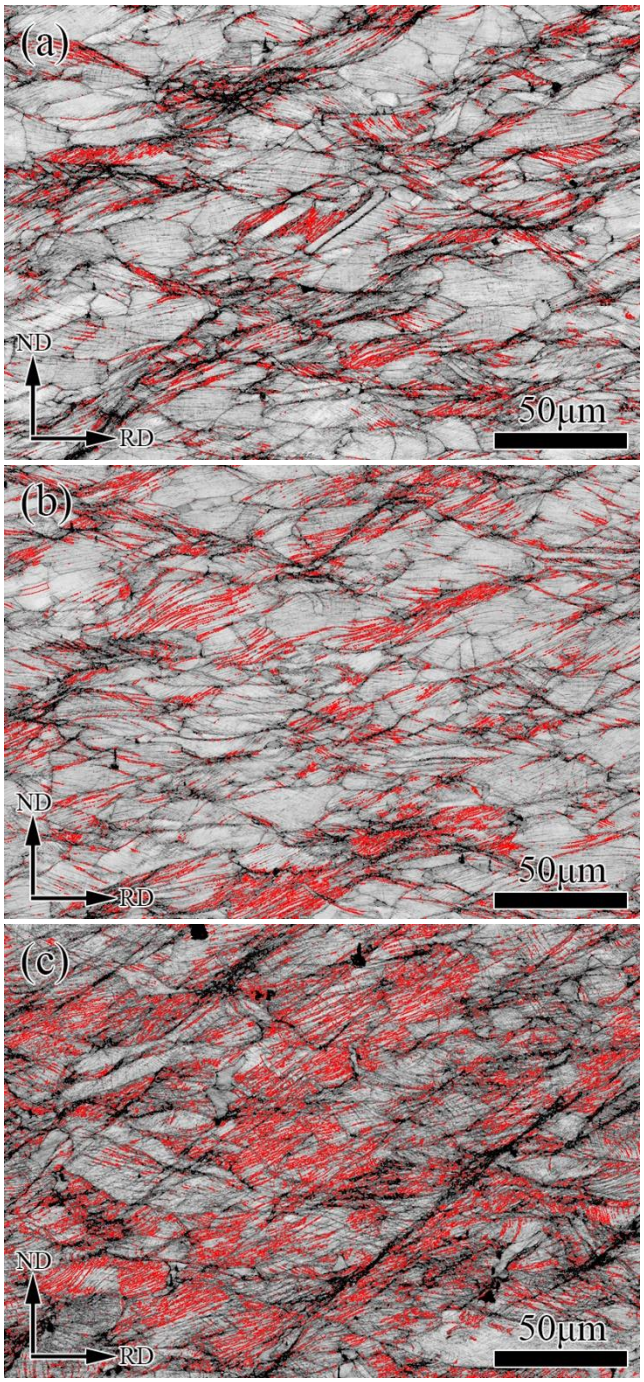

Fig. 2.5 Band contrast maps of the specimens cold-rolled to 50% reduction by (a) 1DR, (b) 1RR and (c) 3RR processes. Twin boundaries are indicated by red lines.

2.3.3 Deformation structure in the late stage of cold rolling

Fig 2.6 shows the SEM-BSE images of the specimens observed from the TD plane after cold rolling to 90% reduction by 1DR, 1RR and 3RR. As reported by Miura *et al.*, the HN structure was formed and the microstructure was inhomogeneous [2.6]. The characteristic eye-shaped deformation twin domains were surrounded by shear bands and further embedded in lamellae. The twinning planes in the twin domains were perpendicular to ND, and the intersections between the twinning plane and TD plane were parallel to RD. Lamellae elongated along the RD. These microstructural features are consistent with those reported in previous reports [2.7, 2.8]. The average area and number density (number of twin domains per unit area) of the twin domains were counted using 50 images with the same magnification, as shown in Fig 2.6. The average twin domain area was $2.3 \pm 0.7\ \mu m^2$, $2.1 \pm 0.9\ \mu m^2$ and $2.2 \pm 1\ \mu m^2$ for 1DR, 1RR and 3RR specimens, respectively. The twin-domain area distributions are shown in Figure 2.7. No significant differences in the average values were observed. Rotational rolling specimens had finer twin domains than unidirectional rolling specimens, and the frequency of coarse twin domains was relatively large; therefore, the rotational rolling specimen had approximately the same average size as the unidirectional rolling specimen. Furthermore, the number density was $0.022 \pm 0.006\ \mu m^{-2}$, $0.028 \pm 0.007\ \mu m^{-2}$ and $0.043 \pm 0.016\ \mu m^{-2}$ for 1DR, 1RR and 3RR specimens, respectively. The number density of the rotationally rolled specimen was larger than that of the unidirectionally rolled specimen. The average area and number density of twin domains were used to determine the area fraction of the twin domains. As a result, the area fraction was 5.0%, 5.9% and 9.5% for 1DR, 1RR and 3RR specimens, respectively. It can be concluded that the rotational rolling process can achieve a finer size and larger area fraction of twin domains than the unidirectional rolling process.

Fig. 2.8 ~ Fig. 2.10 show IPF maps of the 1DR, 1RR and 3RR specimens obtained by SEM-EBSD observations from the TD plane. According to SEM-EBSD observations, the twin domains of HN structures are composed of two different orientation components, i.e., ND // <111> and RD // <211>, or ND // <111> and RD // <110>. These characteristic crystallographic orientations of the twin domains are consistent with those reported previously [2.9].

The texture of the specimens after 90% rolling was measured by X-ray diffraction. After 90% rolling, as shown in the {111} pole figures in Fig. 2.11, the main texture components of all specimens were the same, consisting of Brass{110}<211>, Goss{110}<100>, S{321}<643>, and {111}<110>, {111}<211> (characteristic orientations of the twin domain) orientations. The volume fractions of these orientations were measured using the ODF, and the results are summarized in Fig. 2.12. Compared to unidirectional rolling specimen, rotational rolling specimens contain more twin domains. Moreover, the 3RR specimen with more rotations during cold rolling had the largest volume fraction of twin domains. This result is qualitatively consistent with the SEM-EBSD observations.

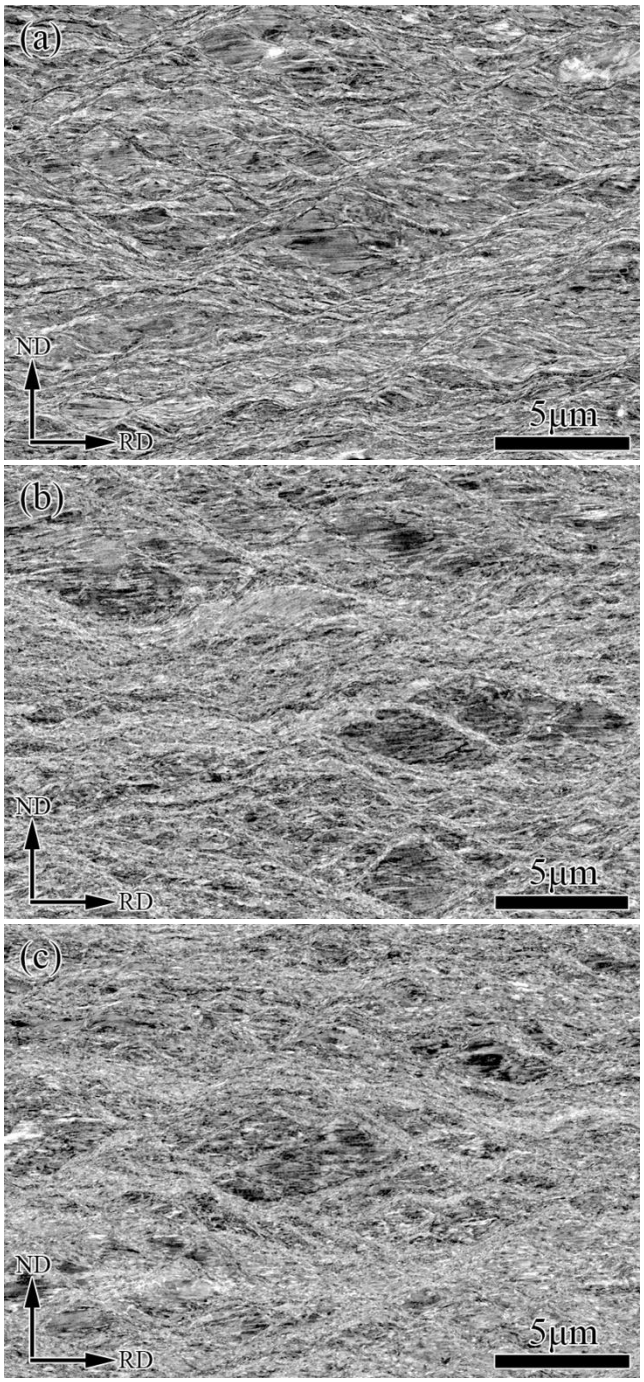

Fig. 2.6 SEM-BSE images of specimens cold-rolled to 90% reduction by (a) 1DR, (b) 1RR and (c) 3RR process.

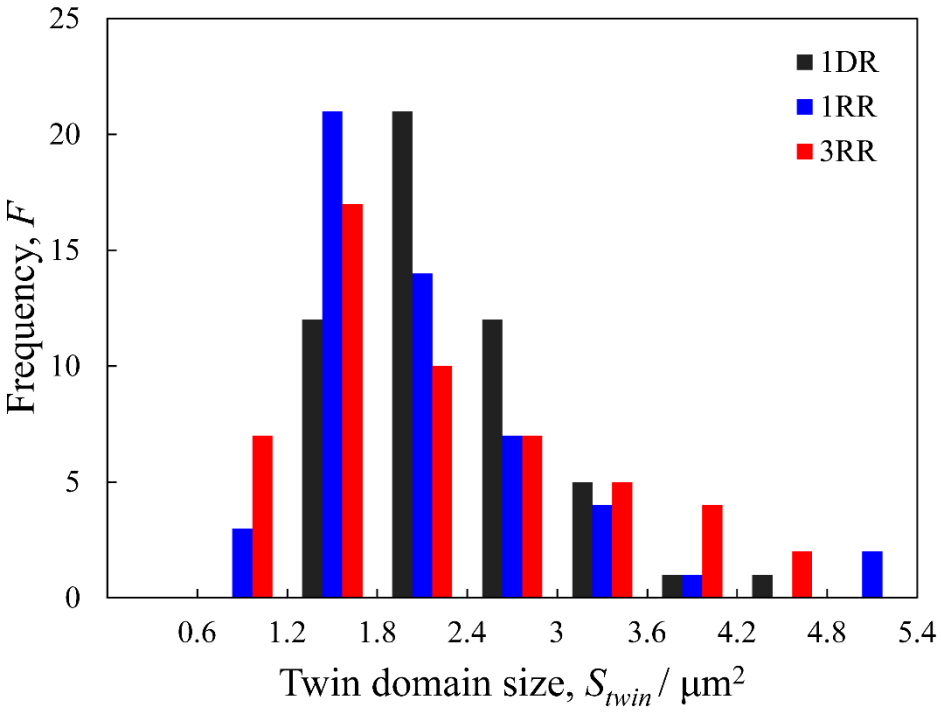

Fig. 2.7 Histograms of the size of twin domains in the specimens cold-rolled to 90% reduction by the 1DR, 1RR and 3RR processes.

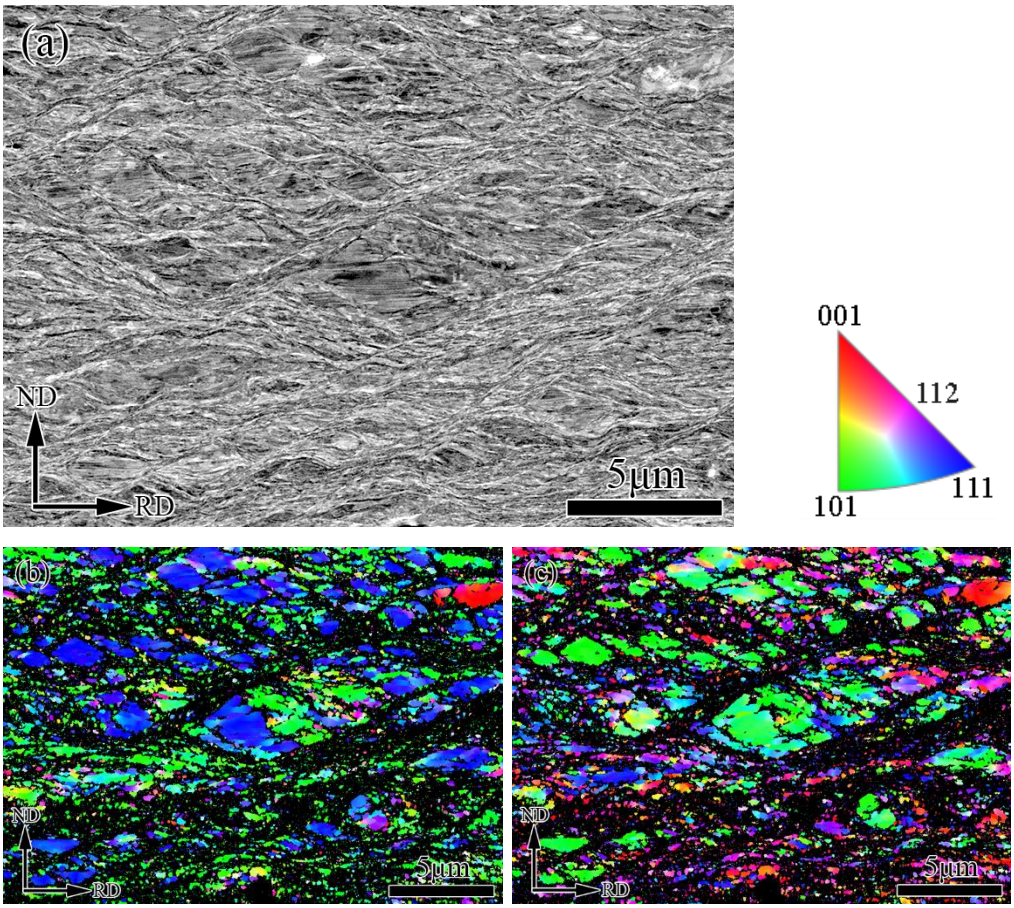

Fig. 2.8 (a) SEM-BSE image of the specimen cold-rolled to 90% reduction by the 1DR process. (b) and (c) Inverse pole figure maps taken in the same area as in (a). Color decoding is parallel to (b) ND and (c) RD.

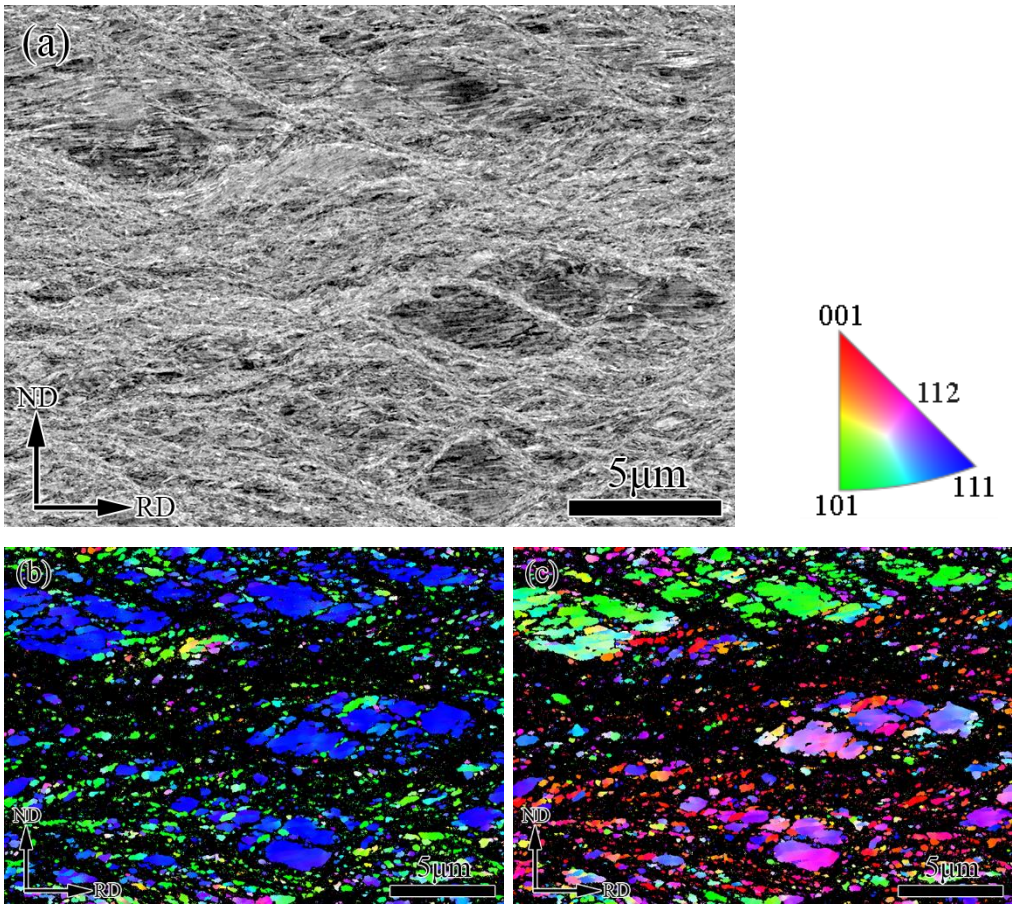

Fig. 2.9 (a) SEM-BSE image of the specimen cold-rolled to 90% reduction by the 1RR process. (b) and (c) Inverse pole figure maps taken in the same area as in (a). Color decoding is parallel to (b) ND and (c) RD.

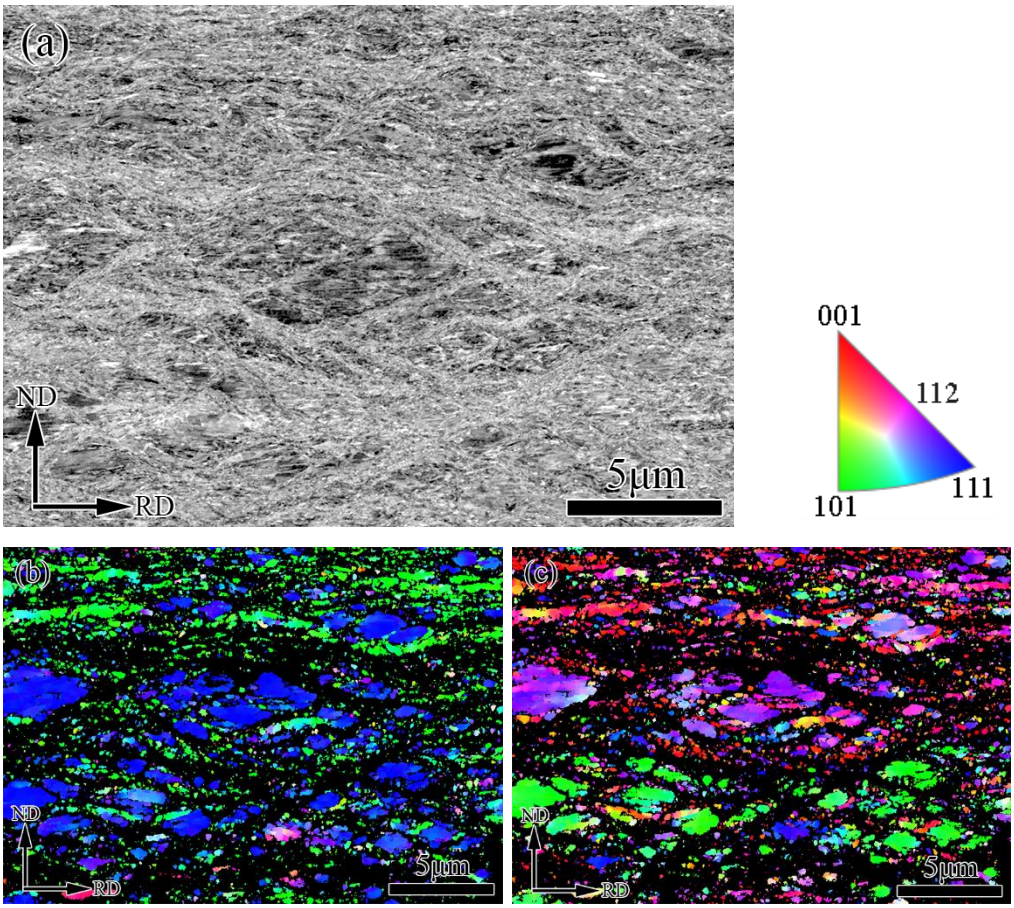

Fig. 2.10 (a) SEM-BSE image of the specimen cold-rolled to 90% reduction by the 3RR process. (b) and (c) Inverse pole figure maps taken in the same area as in (a). Color decoding is parallel to (b) ND and (c) RD.

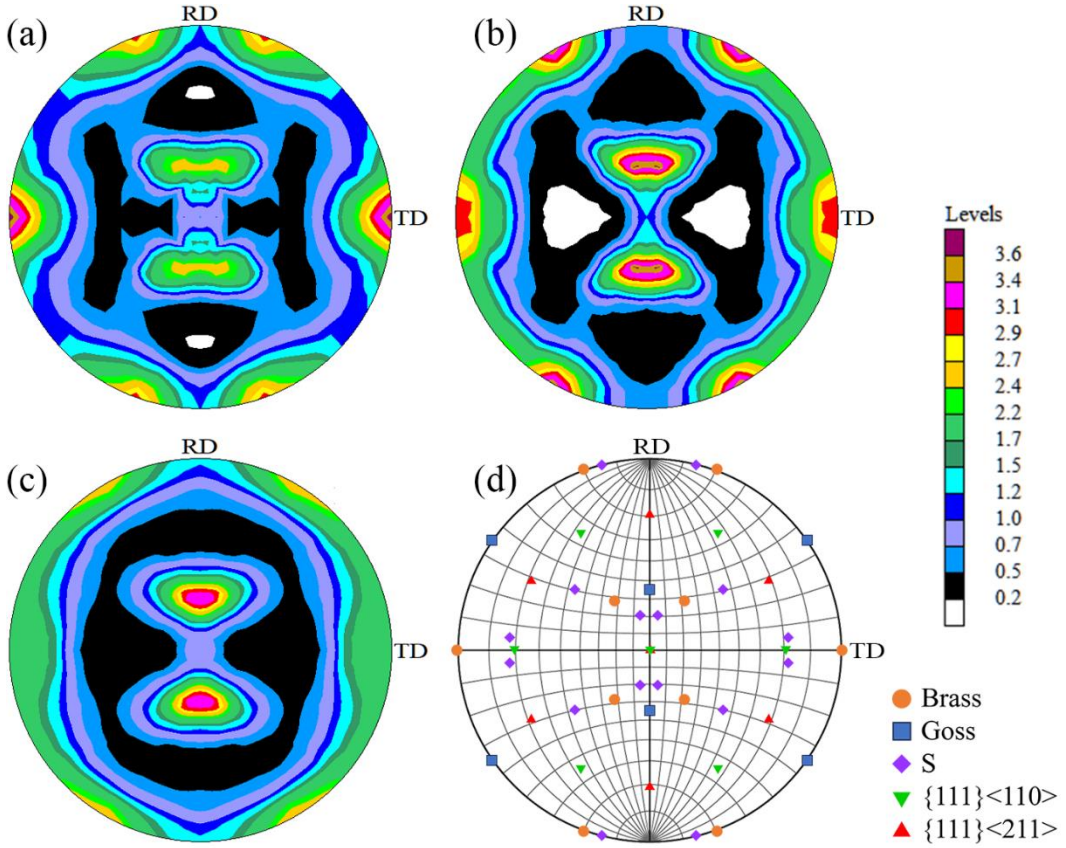

Fig. 2.11 {111} pole figures of the specimens cold-rolled to 90% by (a) 1DR, (b) 1RR and (c) 3RR processes. (d) Main ideal crystallographic orientation of a FCC material in {111} pole figure.

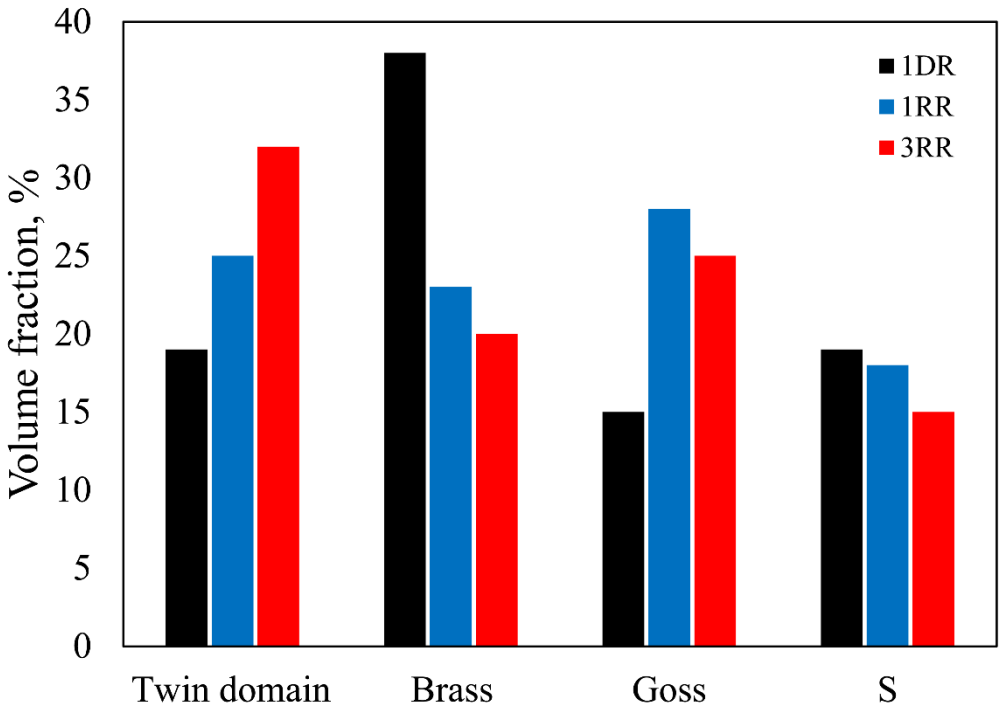

Fig. 2.12 Volume fraction of major texture components in the specimens cold-rolled to 90% reduction by 1DR, 1RR and 3RR processes.

2.3.4 Tensile properties after 90% rolling

Tensile tests were conducted on specimens cold-rolled to 90% reduction by 1DR, 1RR and 3RR. The nominal stress-nominal strain curves are shown in Fig. 2.13. The 0.2% proof stress ($\sigma_{0.2}$), ultimate tensile stress (σ_{UTS}), and fracture strain (ε_f) values are listed in Table 2.2. All the specimens exhibited high strength, which can be attributed to the formation of the HN structure. Notably, the strength-ductility balance of the 3RR specimen was superior to that of the other specimens.

Table 2.2 0.2% proof stress $\sigma_{0.2}$, ultimate tensile strength σ_{UTS}, and fracture strain ε_{f} of the specimens cold-rolled to 90% reduction by 1DR, 1RR and 3RR process.

	$\sigma_{0.2}$ [MPa]	σ_{UTS} [MPa]	ε_{f} [%]
1DR specimen	680±14	750±7	10±0.6
1RR specimen	700±10	770±12	10±1
3RR specimen	740±5	820±6	10±0.6

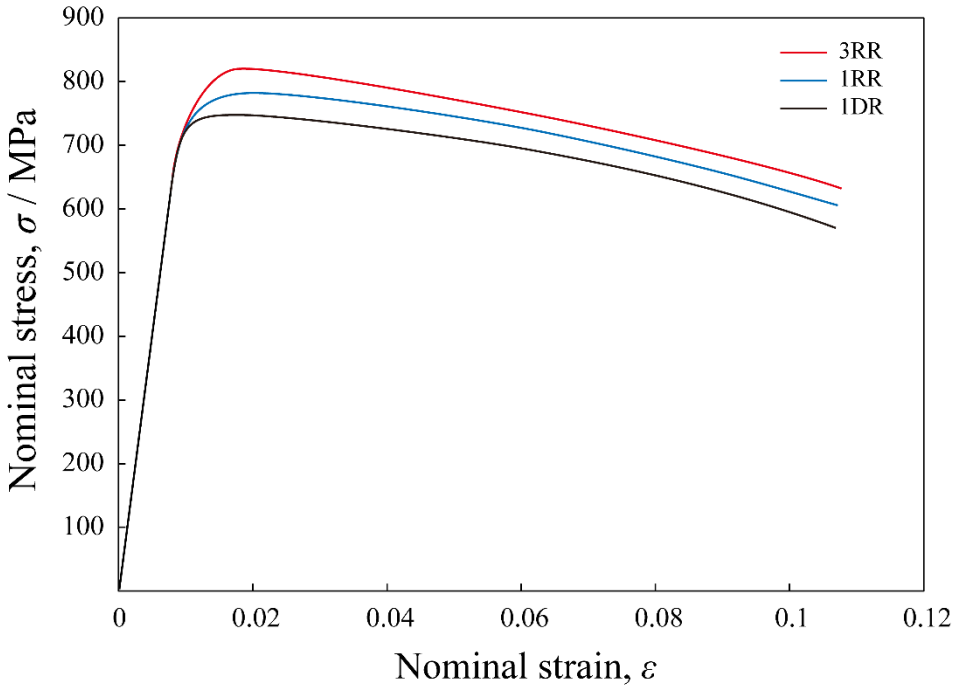

Fig. 2.13 Nominal stress-nominal strain curves of the specimens cold-rolled to 90% reduction by the 1DR, 1RR and 3RR processes.

2.4 Discussion

2.4.1 Effects of rolling process on twin formation at early stage of rolling

As described in Section 2.3.2, the rotational rolling process promotes deformation twinning during the early stage of rolling. Han *et al.* investigated the combined effects of the stacking fault energy, grain size, and crystallographic orientation on deformation twinning. They proposed that the effect of stacking fault energy on deformation twinning decreases with decreasing grain size, while the crystallographic orientation is always related to the ease of deformation twinning [2.10]. Furthermore, the difficulty of mechanical twinning in a grain can be determined by the Schmid factors of twinning and slip systems under externally applied stress conditions. The direction of the applied stress, which maximizes the ratio of the Schmid factor of the twinning system to that of the slip system, is favorable for mechanical twinning [2.11]. Cai *et al.* showed from compression tests of copper single crystals with various orientations that compression along the <001> direction is the most favorable for forming deformation twins, whereas compression along the <111> direction is unfavorable [2.11]. In other words, the formation of deformation twins strongly depends on the crystallographic orientation.

Fig. 2.14 (a) and (b) show the IPF maps obtained by SEM-EBSD observations from the TD plane of the specimens before rolling. Deviations from the <100> and <111> orientations up to ± 15 ° are represented by the same color. Fig. 2.14 (c) shows a band contrast map obtained from an identical area, as shown in Fig. 2.14 (a) and (b) after 10% cold rolling with the rolling plane parallel to the ND plane. In the region shown in the green frame, grains with ND∦<001> but TD ∥ <001> did not form deformation twins after rolling. On the other hand, deformation twins were formed in grains with ND ∥ <001> in the yellow-frame region. Fig. 2.15 shows the IPF maps and band contrast map, but it is different from Fig. 2.14, that is, the rolling plane parallel to the TD plane. Deformation twins were observed in grains with an ND∦<001> orientation but a TD ∥ <001> orientation, as shown in the green frame. The grain with the TD ∥ <111> orientation, shown in the yellow frame, did not form deformation twins. Although the processing method employed in the present study differs from compression tests, analyses of the deformation structure were performed at the half-thickness part of the rolled plate, where the deformation mode was assumed to be similar to that of compression. These results are qualitatively consistent with the conclusions of Cai *et al*.

Therefore, mechanical twinning should occur even in grains with orientations in which it is difficult to form deformation twins in the 1DR process by varying the rolling plane during the rotational rolling process. With this mechanism, it is understandable that the number of grains containing deformation twins increased by the rotational rolling process.

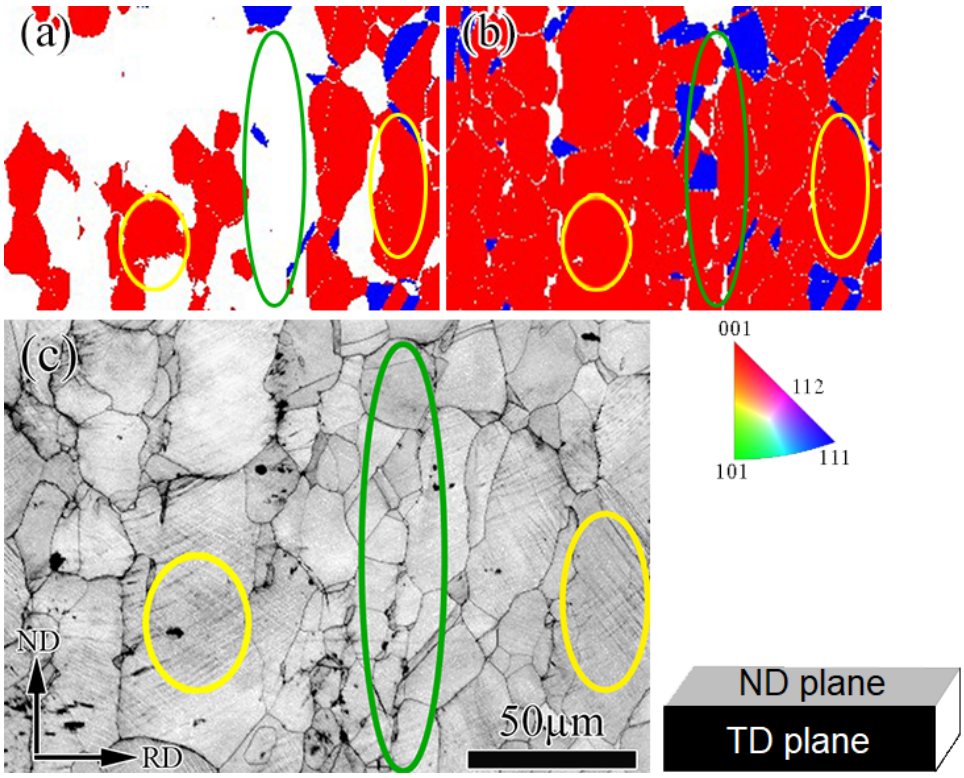

Fig. 2.14 (a) and (b) Inverse pole figure maps of the specimen before rolling. Color decoding is parallel to the (a) ND and (b) TD. (c) SEM-BSE image taken in the same area as (a) and (b) after 10% cold rolling. The rolling surface was parallel to the ND plane.

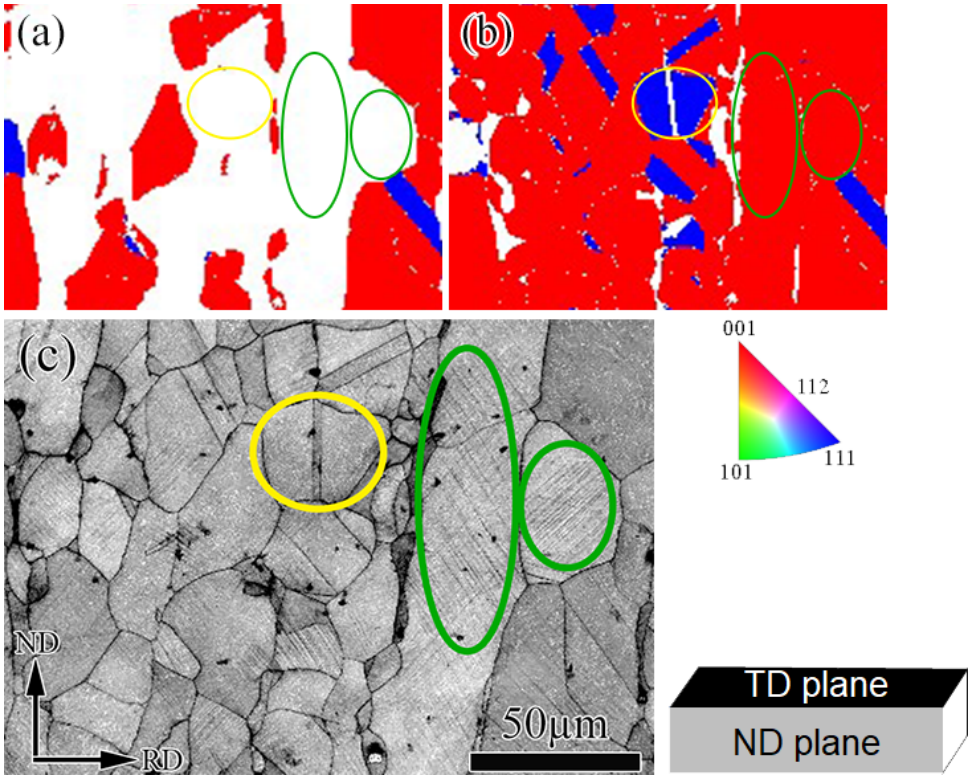

Fig. 2.15 (a) and (b) Inverse pole figure maps of the specimen before rolling. Color decoding is parallel to the (a) ND and (b) TD. (c) SEM-BSE image taken in the same area as (a) and (b) after 10% cold rolling. The rolling surface was parallel to the TD plane.

2.4.2 Effects of rolling process on formation of twin domains in the HN structure

The rotational rolling process can increase the number of deformation twins introduced into the initial coarse grains by changing the rolling plane and promoting the formation of twin domains derived from the deformation twins. In addition, the rotational rolling process can refine the size of the twin domains (Fig. 2.7). Twin domains were previously reported to form through the subdivision of deformation twins developed in the initial coarse grains by shear bands [2.9], and shear bands preferentially formed in regions with a high density of deformation twins [2.12]. Therefore, the rotational rolling process promoted mechanical twinning at the early stage of rolling, increasing the number of shear bands and leading to refinement of the twin domains.

The lowering of the stacking fault energy of alloys by adjusting their composition has received attention as a way to control the HN structure; however, this study shows that the HN structure and mechanical properties can be controlled by modifying the fabrication process, even in identical alloys. Therefore, advancements in the processing methods may result in new developments in the control of HN structures.

2.4.3 Effects of rolling process on the tensile properties

The improvement in the strength-ductility balance of the rotational rolling process can be attributed to the increased volume fraction of the twin domains (Fig. 2.12). Aoyagi *et al.* [2.1] used a crystal plasticity simulation to investigate the deformation behavior of an HN-structured stainless steel and found that plastic deformation occurred preferentially in the shear bands and then propagated into the twin domains. Furthermore, they predicted that increasing the volume fraction of the twin domains in the HN structure would improve the strength. In this study, the 1RR and 3RR specimens with a larger twin domain volume fraction exhibited higher strength than the 1DR specimen, which is qualitatively consistent with the results of Aoyagi *et al.* [2.1]. Park *et al.* [2.13] investigated the tensile properties of ferrite-martensite dual-phase steels with various distributions of the hard martensite phase and found that as the hard phase was finely dispersed when its volume fraction was constant, the strength increased without a decrease in elongation. Moreover, the local elongation slightly increased, whereas the strength significantly increased. The HN structures in the present specimens were different from those of the ferrite-martensite duplex structures; however, based on the findings of Aoyagi *et al.* [2.1], the twin domain can be considered a hard region. Therefore, the strength and local elongation of the rotationally rolled specimen would be improved owing to the fine dispersion of the twin domains. Furthermore, Miura *et al.* demonstrated that the development of twin domains in HN structures prevents the development of a sharp rolling texture, thereby improving the strength-ductility balance [2.14]. In conclusion, the combined effects of the increase in the volume fraction of the twin domains and refinement in its size resulted in an improved strength-ductility balance in the rotational rolling process.

2.5 Conclusion

The microstructure and mechanical properties of a Cu-37.75 mass% Zn-0.11 mass% Sn alloy subjected to unidirectional rolling (1DR) and rotational rolling (1RR and 3RR) were investigated. The main results obtained are summarized as follows:

(1) At a 50% reduction, the frequency of grains with deformation twins in the rotationally rolled specimens was higher than that in the 1DR specimen. The rotational rolling process, i.e., a change in the rolling plane, promoted mechanical twinning within grains with crystallographic orientations that were difficult to form by the 1DR process.

(2) At 90% reduction, HN structures consisting of twin domains, shear bands and lamellar grains were fully developed in both rolling conditions. In the rotational rolling specimens, the volume fraction and size of the twin domains were larger and finer, respectively, than those of the 1DR specimen.

(3) The rotationally rolled specimens at 90% reduction exhibited a better strength-ductility balance than the 1DR specimen. It was strongly suggested that an increase in the volume fraction of the twin domains effectively improved the strength-ductility balance.

In summary, changing the rolling plane significantly affected the formation of the HN structure, as well as the mechanical properties. In other words, the HN structure is controlled by the influence of the crystallographic orientation on mechanical twinning. Improvements in the fabrication processes based on the crystallographic orientation can be developed as a new method for controlling the HN structure.

Reference

[2.1] Y. Aoyagi, C. Watanabe, M. Kobayashi, Y. Todaka and H. Miura: Tetsu-to-Hagane, 2019, 105(2), 140-149.

[2.2] C. Watanabe, S. Kobayashi, Y. Aoyagi, Y. Todaka, M. Kobayashi, N. Sugiura, N. Yoshinaga and H. Miura: ISIJ Int., 2020, 60(3), 582-589.

[2.3] P. Yang, Q. Xie, L. Meng, H. Ding, and Z. Tang: Scr. Mater., 2006, 55(7), 629-631.

[2.4] L. Meng, P. Yang, Q. Xie, H. Ding, and Z. Tang: Scr. Mater., 2007, 56(11), 931-934.

[2.5] J.A. Bearden: Rev. Mod. Phys., 1967, 39(1), 78.

[2.6] H. Miura, Y. Takahashi, H. Yamaguchi and K. Kamibayashi: J. Japan Inst. Copper, 2010, 49(1), 51-55.

[2.7] H. Miura, M. Kobayashi, I. Maki, H. Mori and Y. Ito: J. Japan Inst. Copper, 2016, 55(1), 190-196.

[2.8] H. Miura, M. Kobayashi, Y. Todaka, C. Watanabe, Y. Aoyagi, N. Sugiura and N. Yoshinaga: Scr. Mater., 2017, 133, 33-36.

[2.9] C. Watanabe, S. Kobayashi, Y. Aoyagi, Y. Todaka, M. Kobayashi, N. Sugiura, N. Yoshinaga and H. Miura: ISIJ Int., 2020, 60(3), 582-589.

[2.10] W.Z. Han, Z. F. Zhang, S.D. Wu and S.X. Li: Philos. Mag., 2008, 88(24), 3011-3029.

[2.11] S.S. Cai, X.W. Li and N.R. Tao: J. Mater. Sci. Technol., 2018, 34(8), 1364-1370.

[2.12] G.H. Xiao, N.R. Tao, K. Liu: Mater. Sci. Eng. A, 2009, 513, 13-21.

[2.13] K. Park, M. Nishiyama, N. Nakada, T. Tsuchiyama, S. Takaki: Mater. Sci. Eng. A, 2014, 604, 135-141.

[2.14] H. Miura, M. Kobayashi, Y. Todaka, C. Watanabe, Y. Aoyagi: J. Japan Inst. Metals, 2017, 81(12), 536-541.

Chapter III Effects of initial orientation in normal direction on the development of heterogeneous-nano structure and mechanical properties in a Cu-Zn system alloy

3.1 Introduction

In Chapter II, it was found that deformation twinning in the Cu-Zn alloy was promoted at the initial rolling stage by subjecting it to rotational rolling, in which the rolling surface was 90° rotated with a fixed rolling direction. The cause of the above results was explained by the formation of deformation twins in the initial coarse grains having a crystallographic orientation along the ND parallel not to <001> and the TD parallel to <001> by rotational rolling. In contrast, mechanical twinning scarcely occurred in these grains owing to simple unidirectional rolling. Moreover, it has been reported that the formation of deformation twins depends strongly on the crystallographic orientation in the loading direction. Cai *et al*. investigated the orientation dependence of mechanical twinning through compression tests on pure copper single crystals with different orientations. They showed that specimens with the <001> direction parallel to the compression axis were most prone to twinning [3.1]. Karaman *et al*. investigated the relationship between the activated deformation mechanisms and crystallographic orientation of a Fe-12.34mass%Mn-1.03mass%C alloy during unidirectional tension and compression. They demonstrated that mechanical twinning was activated as the primary deformation mechanism in grains with a <001> direction parallel to the loading direction in compression, but along the <111> direction in tension [3.2].

These experimental results strongly suggest that the initial orientation in the normal direction of rolling is essential for mechanical twinning. The present study systematically investigated the effects of the initial orientation along the ND on the formation of deformation twins in the Cu-Zn alloy during cold rolling. In addition, the influence of the initial orientation on the evolved HN structure and its mechanical properties is discussed.

3.2 Experimental procedure

The same hot-extruded rods of commercial Cu-Zn-Sn alloy were used as described in Chapter II. Two types of specimens were cut from the rod using a wire electric discharge machine, as shown in Fig. 3.1. The specimens were unidirectionally rolled to a maximum thickness reduction of 90% at room temperature.

The experimental conditions for texture measurements, microstructural observations, and tensile tests were the same as those in Chapter II.

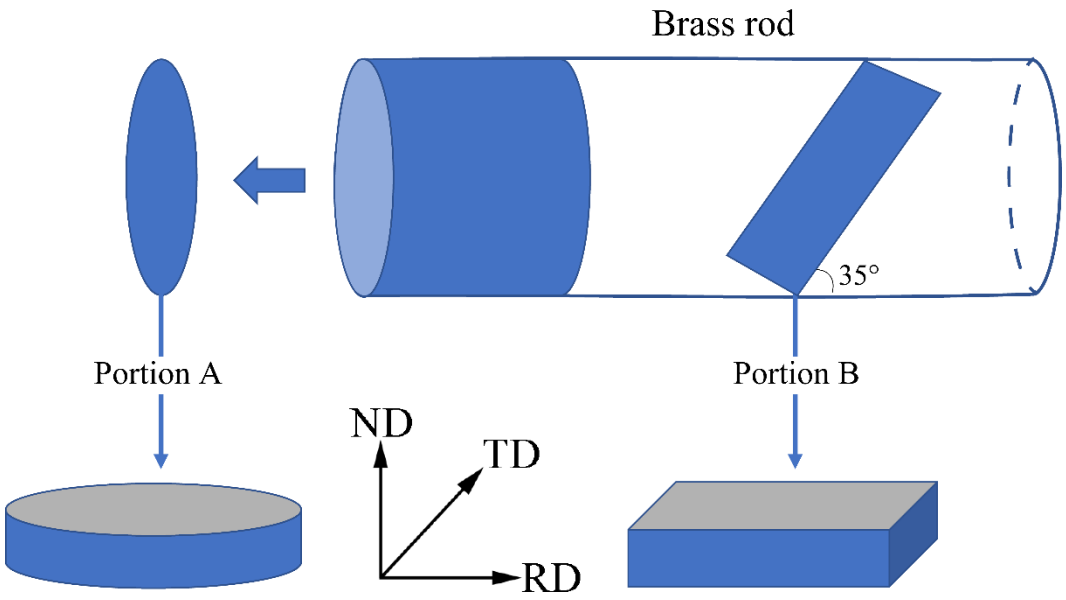

Fig. 3.1 Schematic illustration showing the preparation of specimens with different textures. The portion A has a strong <001> texture along the ND and the portion B has <111> texture.

3.3 Results

3.3.1 Initial texture

The initial textures of the specimens are shown in Fig. 3.2. The specimen indicated as portion A in Fig. 3.1 exhibits a strong <001> texture on the ND plane (Fig. 3.2 (a)). On the other hand, the specimen indicated as portion B, in which the cutout direction is inclined at 35.26° from the extrusion direction, possesses a relatively substantial accumulation of <111> components on the ND plane (Fig. 3.2 (b)). Hereafter, the former and latter specimens are referred to as <001> and <111> specimens, respectively.

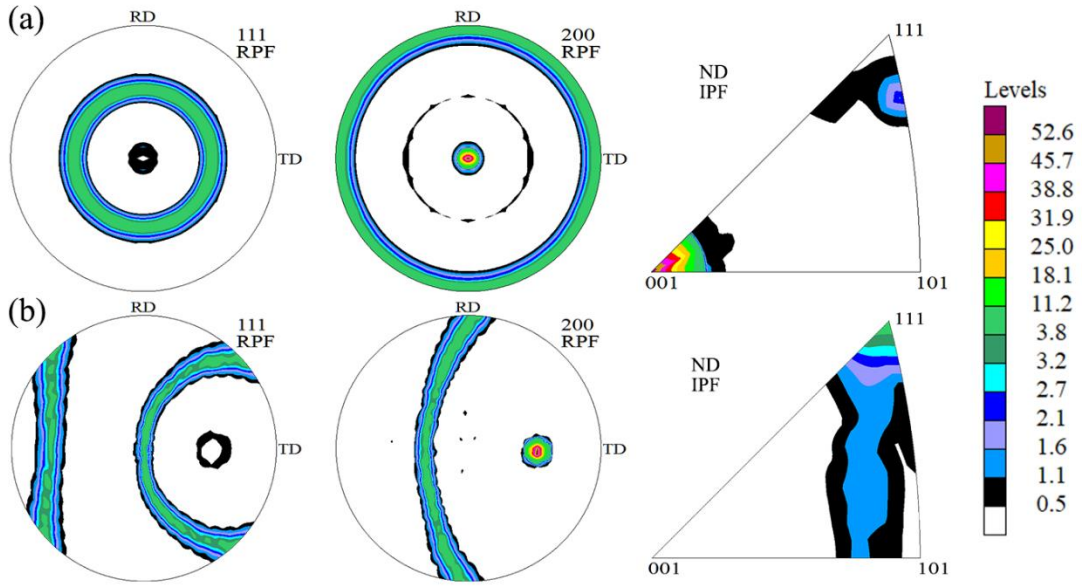

Fig. 3.2 {111} and {200} pole figures and inverse pole figures of the ND plane of specimens (a) < 001 > and (b) < 111 >.

3.3.2 Microstructure at the intermediate stage of cold rolling

Fig. 3.3 shows the band contrast maps of the two specimens after cold rolling to a 50% reduction. The red lines on the map indicate twin boundaries (Σ3 grain boundaries). In both specimens, deformation twins formed in the initial coarse grains. The <001> specimen comprises denser twin boundaries than the <111> one. For quantitative evaluation, the ratio of the number of twinned grains to the whole grains was determined in the specimens cold-rolled to 10, 30, and 50% thickness reductions. The results are summarized in Fig. 3.4. At the initial stage of rolling (10%), the ratio in the <001> specimen was more significant than that in the <111> one. After 30% reduction, the difference in the values between the two specimens increased. After 50% reduction, the ratio in the <111> specimen increased notably. However, the difference in values between the two specimens remained unchanged. Not all twin boundaries can be detected by EBSD analyses because cold rolling introduces high densities of lattice defects and crystallographic orientation changes among the twins. Therefore, the ratio of grains containing twins was underestimated. However, because EBSD analyses were conducted on both specimens under identical observation conditions (such as acceleration voltage and step size), the fraction of twinned grains in the <001> specimen was higher than that in the <111> one.

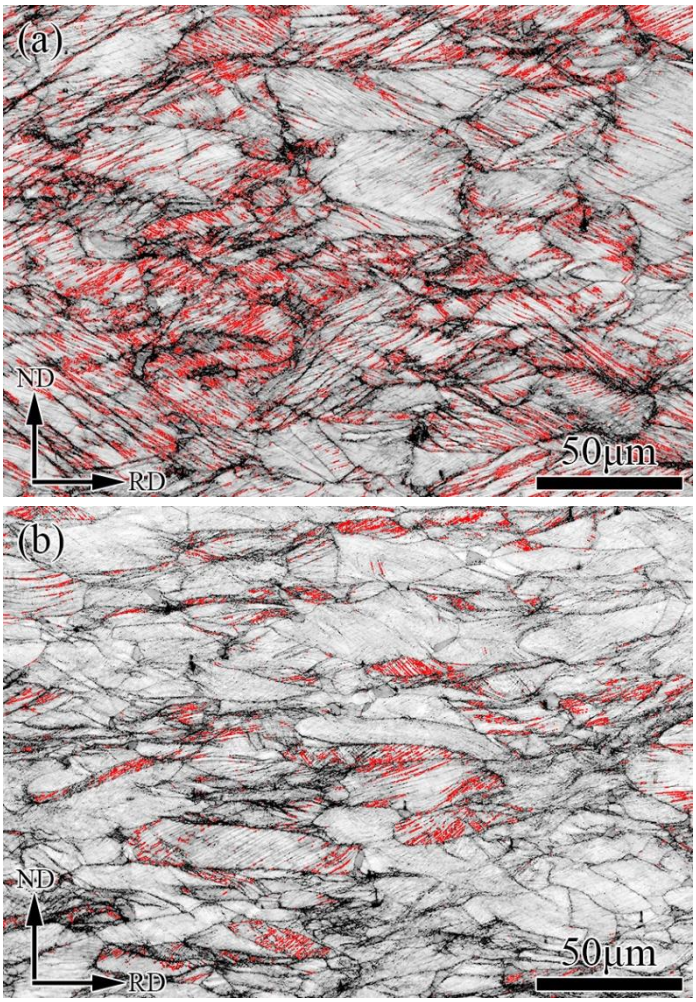

Fig. 3.3 Band contrast maps of (a) <001> and (b) <111> specimens cold-rolled to 50% reduction. The red lines indicate the twin boundaries.

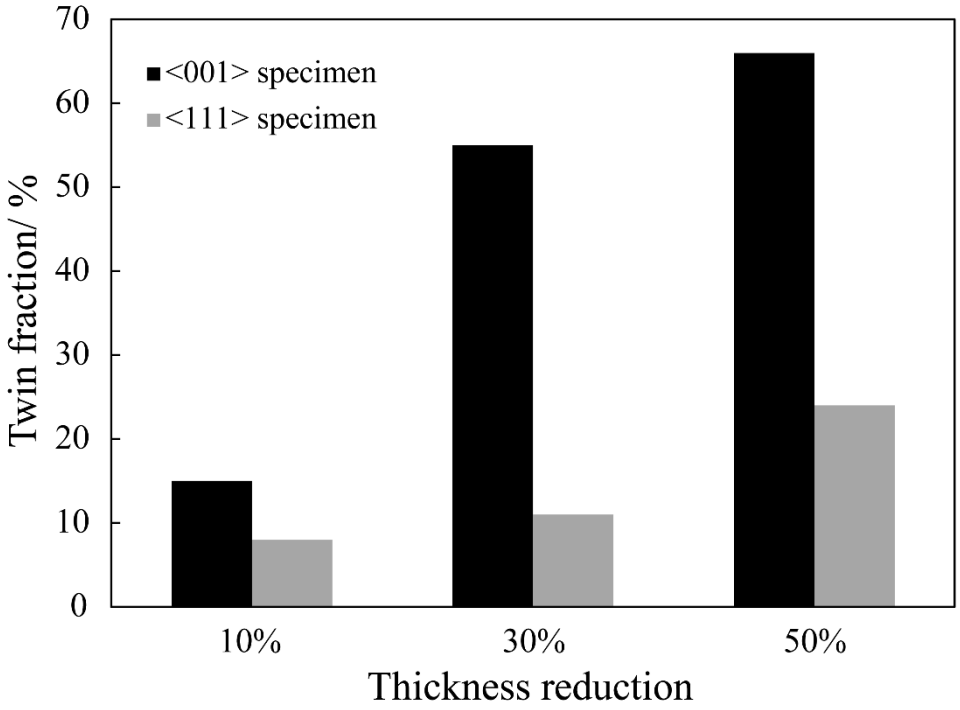

Fig. 3.4 The twin fraction of <001> and <111> specimens cold-rolled to 10%, 30% and 50% reduction.

3.3.3 Microstructure at the later stage of cold rolling

Fig. 3.5 shows the BSE images of the two specimens cold-rolled to a 90% reduction. The HN structure with twin domains was observed in both specimens. The twin domains are indicated by the arrows in Fig. 3.5. The twin domains were surrounded by shear bands and embedded in lamellar grains. As mentioned in Section 2.3.3, there are two types of twin domains with crystallographic orientations of i) <111> // ND, <110> // TD, and ii) <111> // ND, <211> // TD. The characteristics of the HN structure were consistent with those reported in previous studies [3.3, 3.4].

Fig. 3.6 shows the {111} pole figures of the <001> and <111> specimens after 90% cold rolling. The <001> specimen possesses a higher intensity of ND // {111} texture than the <111> one. The volume fraction of the ND // <111>, RD // <211>, or ND // <111>, RD // <110> components, which comprise twin domains, were estimated by analyzing the ODF. The estimates were 24% and 20% for the <001> and <111> specimens, respectively.

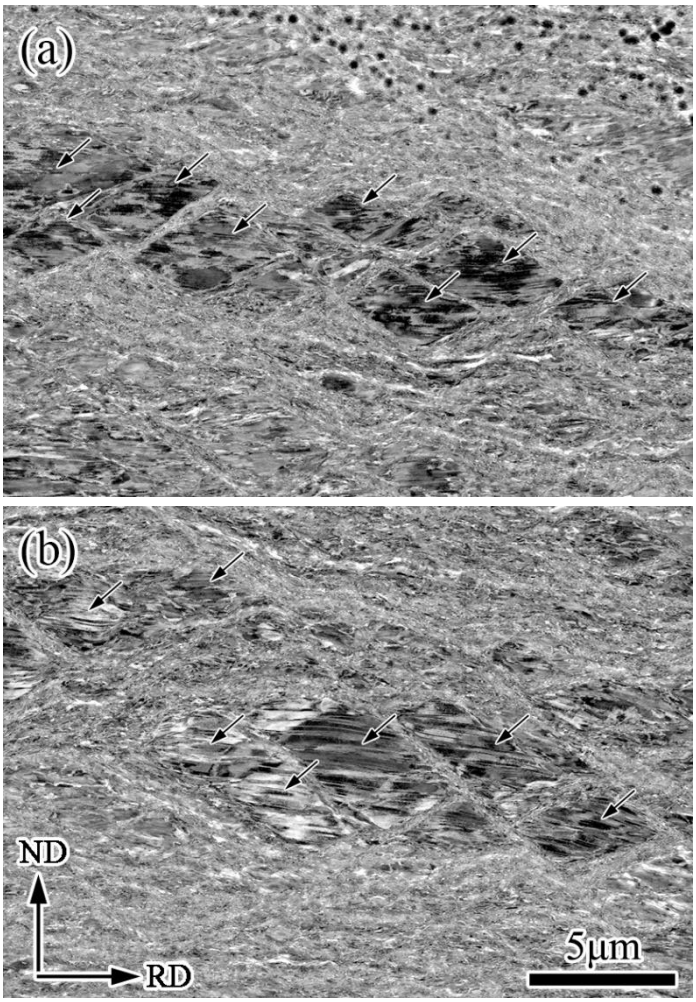

Fig. 3.5 SEM-BSE images of (a) <001> and (b) <111> specimens cold-rolled to 90% reduction.

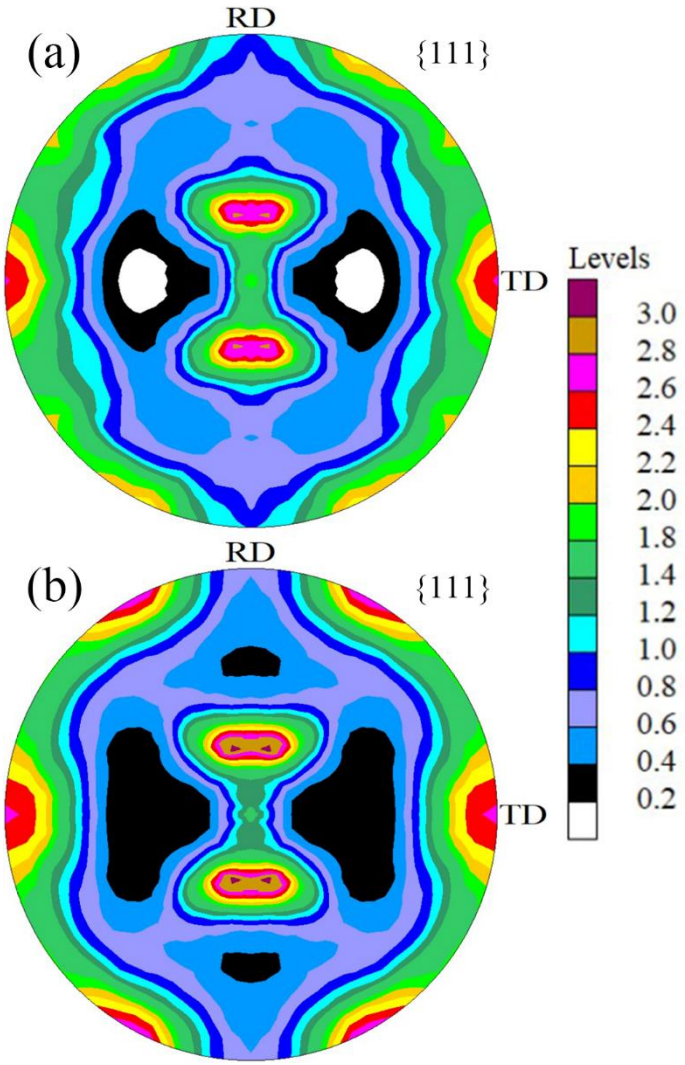

Fig. 3.6 {111} pole figures of the (a) <001> and (b) <111> specimens cold-rolled to 90% reduction.

3.3.4 Evolution of crystallographic orientation during rolling

Fig. 3.7 shows the changes in the inverse pole figures along the ND of the <001> and <111> specimens with an increase in the rolling reduction. Cold rolling caused a rotation of the crystallographic orientation in both specimens. In the <001> specimen, the ND // <001> component decreased during rolling up to a 50% reduction, whereas the ND // <111> component increased after a 70% reduction, which did not exist before rolling. In contrast, in the <111> specimen, the intensity of the ND // <111> component decreased with increasing rolling reduction and then increased slightly after 70% rolling. The ND // <011> and ND // <111> components became the primary orientations in both the specimens after 90% rolling. The former corresponds well to the crystallographic feature of the lamellar grains developed in the HN structure [3.3] and the latter to the "eye-shaped" twin domains, as described in Section 3.3.3. Thus, the terminal textures in both specimens were almost identical, owing to the formation of the HN structure. However, the evolution process was considerably different.

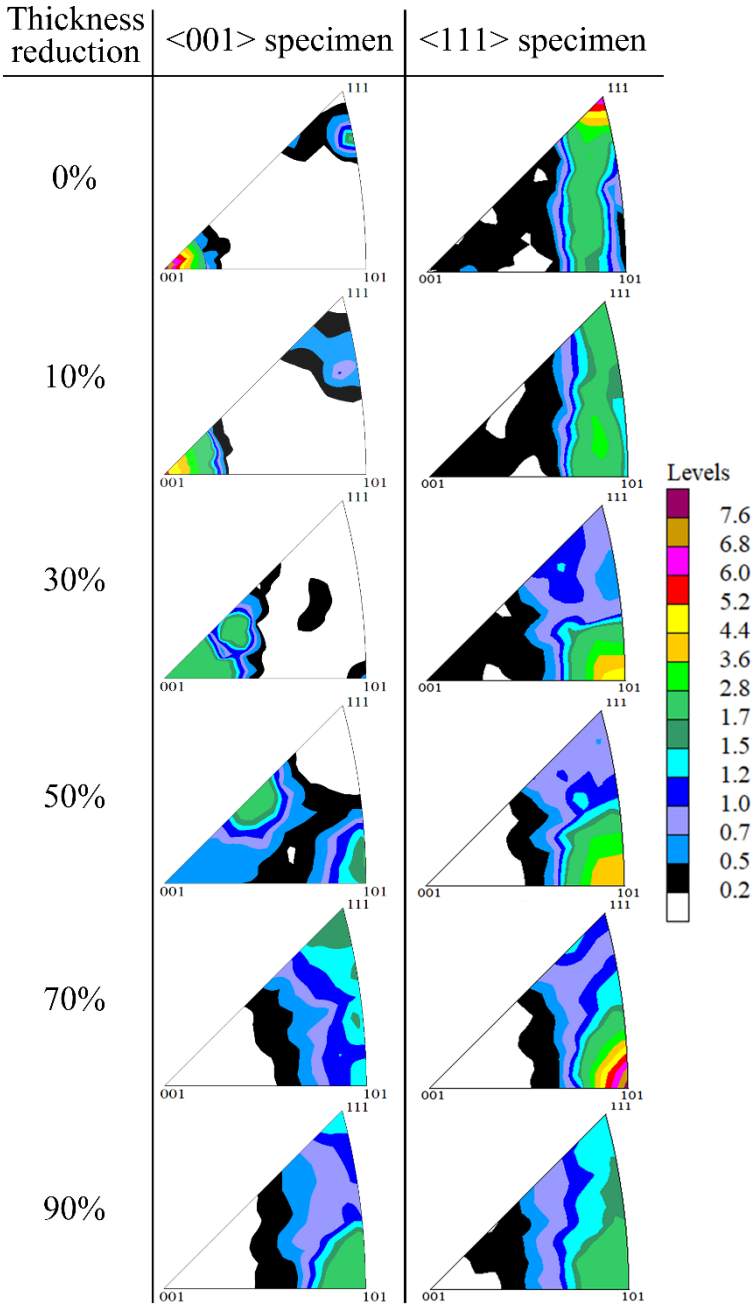

Fig. 3.7 Inverse pole figures along the ND of the <001> and <111> specimens cold-rolled to a thickness reduction of 0%-90%.

3.3.5 Tensile properties of specimens cold-rolled to 90% reduction

Fig. 3.8 shows the nominal stress-nominal strain curves of both specimens after 90% cold rolling. The values of the 0.2% proof stress ($\sigma_{0.2}$), ultimate tensile stress (σ_{UTS}), and fracture strain (ε_f) are listed in Table 3.1. Both specimens exhibited high strength, which can be attributed to the formation of the HN structure [3.5]. However, the strength-ductility balance of the <001> specimen was superior to that of the <111> specimen.

Table 3.1 0.2% proof stress $\sigma_{0.2}$, ultimate tensile strength σ_{UTS}, and fracture strain ε_f of <001> and <111> specimens cold-rolled to 90% reduction.

	$\sigma_{0.2}$ [MPa]	σ_{UTS} [MPa]	ε_f [%]
<001> specimen	730±20	790±6	12±1
<111> specimen	695±13	730±6	8±1

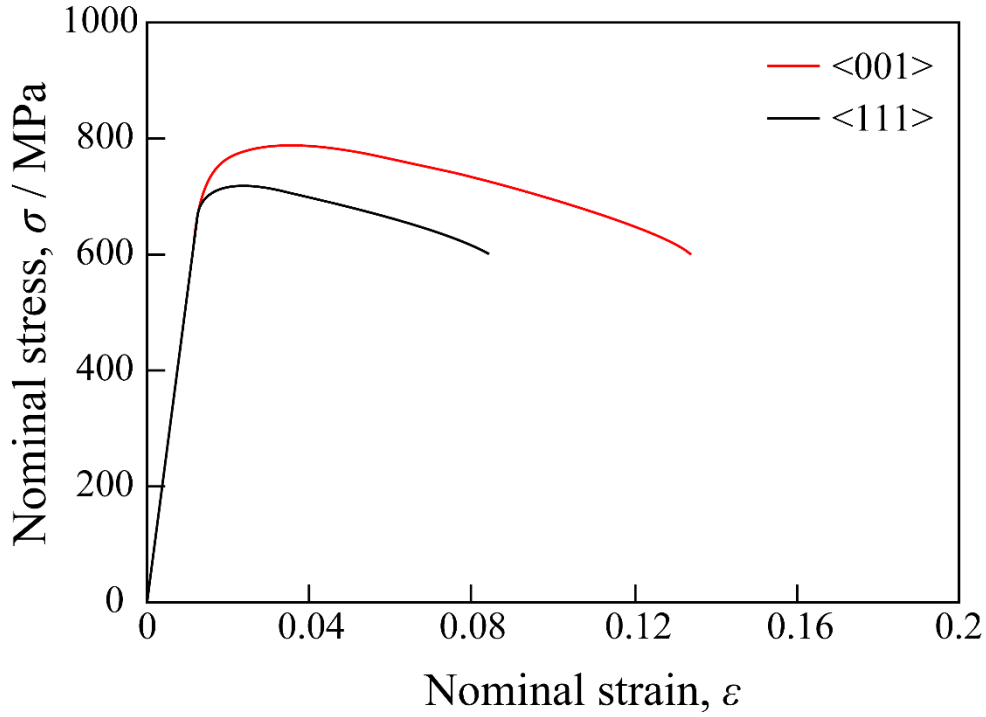

Fig. 3.8 Nominal stress-nominal strain curves of the <001> and <111> specimens cold-rolled to 90% reduction.

3.4 Discussion

3.4.1 Effects of initial orientation in ND on microstructure development during cold rolling

As discussed in Chapter III, the difficulty of mechanical twinning in a grain can be determined by the ratio of the maximum Schmid factor of the twinning system (m_T) to that of the slip system (m_S) [3.1]. The m_T / m_S of grains with ND // <001> was much larger than that of grains with the ND // <111> orientation. Thus, the frequency of mechanical twinning during cold rolling was higher in the <001> specimens, which had a relatively higher volume fraction of grains with ND // <001> (Fig. 3.3 and 3.4). The deformation twin domains in the HN structure originate from twinned grains that develop during cold rolling [3.3]. Therefore, it can be reasonably understood that more deformation twins could be introduced in the <001> specimen to evolve a higher volume fraction of twin domains in the HN structure than that in the <111> specimen.

The ND // <111> component increased in both specimens with rolling reduction from 50 to 70% (Fig. 3.7). This increase can be attributed to the formation of twin domains, as described in Section 3.3.3. Watanabe *et al.* systematically investigated the formation process of HN structure. They reported that the twinned coarse grains were subdivided by shear bands to form twin domains with increasing rolling reduction, and eventually transitioned to lamellar structures [3.3]. The intensity of the ND // <111> component in the <001> specimen was lower at a 90% rolling reduction than at 70% (Fig. 3.7). This indicates that the volume fraction of twin domains was smaller at 90% than at 70%. As discussed in Section 3.4.2, the volume fraction of twin domains in the HN structure strongly affects the mechanical properties. Moreover, as mentioned in Section 3.3.4, the evolution of the texture during rolling differed significantly between the two specimens. Therefore, it is strongly suggested that an appropriate rolling reduction exists depending on the initial texture to optimize the mechanical properties.

3.4.2 Effects of initial orientation in ND on mechanical properties of heavily cold-rolled specimens

Aoyagi *et al*. investigated the deformation behavior of HN-structured materials using a crystal plasticity simulation. They suggested that the tensile strength of HN-structured materials increased with increasing volume fraction of the "eye-shaped" deformation twin domains [3.5]. In the present study, the tensile strength of the <001> specimen, which had a higher volume fraction of twin domains, was higher than that of the <111> specimen. This finding was qualitatively consistent with the results reported by Aoyagi *et al*.

Miura *et al*. reported that the evolution of deformation twin domains in the HN structure suppresses the formation of a strong rolling texture to improve ductility [3.6-3.8]. Thus, the <001> specimen with a higher volume fraction of deformation twin domains possesses a more significant elongation and higher tensile strength than the <111> one. However, the relationship between the ratio of each component structure in the HN structure ("eye-shaped" deformation twin domains, shear bands, and lamellae) and ductility is not yet fully understood; hence, further study is necessary.

As discussed above, the initial texture significantly affected the morphology of the terminal HN structure and the mechanical properties of the specimens because of the frequency of deformation twinning during the early rolling stage. To date, the HN structure has been controlled mainly by adding alloying elements to change the SFE of alloys. However, in the present study, it was revealed that the characteristics of the HN structure could be modified even in an identical alloy by controlling the initial texture and improving the mechanical properties of the alloy. Moreover, depending on the initial texture, an optimum rolling reduction exists for the development of the HN structure. Improvements in the manufacturing process based on the knowledge obtained in this study are expected to enhance the mechanical properties of HN-structured materials.

3.5 Conclusion

Two specimens with different initial orientations in the ND were prepared from a Cu-37.75mass%Zn-0.11mass%Sn alloy bar. The specimens were subjected to heavy cold rolling to investigate the effects of the initial texture on the evolution of their microstructure and mechanical properties. The results are summarized as follows:

(1) From the initial to intermediate stage of rolling (10 to 50% reduction in thickness), the ratio of twinned grains to whole grains in the specimen with a strong <001> texture parallel to the plane normal of the specimen (<001> specimen) was higher than that in the one with <111> texture (<111> specimen).

(2) Heterogeneous-nanostructure comprising “eye-shaped” twin domains, shear bands, and conventional lamellae were formed in both specimens after 90% cold rolling. The volume fraction of twin domains was higher in the <001> specimen than in the <111> one.

(3) After 90% rolling, the <001> specimen exhibited a higher strength-ductility balance than the <111> specimen.

In summary, the initial texture significantly influences the evolution of the HN structure after heavy cold rolling and its mechanical properties. Optimizing the initial texture can promote the development of the heterogeneous nano structure. Thus, further improvements in mechanical properties can be achieved.

Reference

[3.1] S.S. Cai, X.W. Li and N.R. Tao: J. Mater. Sci. Technol., 2018, 34(8), 1364-1370.

[3.2] I. Karaman, H. Sehitoglu, K. Gall, Y.I. Chumlyakov and H.J. Maier: Acta Mater., 2000, 48(6), 1345-1359.

[3.3] C. Watanabe, S. Kobayashi, Y. Aoyagi, Y. Todaka, M. Kobayashi, N. Sugiura, N. Yoshinaga and H. Miura: ISIJ Int., 2020, 60(3), 582-589.

[3.4] Y. Li, N. Koga, C. Watanabe and H. Miura: Mater. Trans., 2022, 63(4), 497-501.

[3.5] Y. Aoyagi, C. Watanabe, M. Kobayashi, Y. Todaka and H. Miura: Tetsu-to-Hagane, 2019, 105(2), 140-149.

[3.6] H. Miura, M. Kobayashi, Y. Todaka, C. Watanabe, Y. Aoyagi: J. Japan Inst. Metals, 2017, 81(12), 536-541.

[3.7] H. Miura, M. Kobayashi, Y. Todaka, C. Watanabe, Y. Aoyagi, N. Sugiura and N. Yoshinaga: Scr. Mater., 2017, 133, 33-36.

[3.8] H. Miura, Y. Iwama and M. Kobayashi: Mater. Trans., 2019, 60(7), 1111-1115.

Chapter IV Effects of initial orientation in rolling direction on the mechanical twinning in a Cu-Zn system alloy

4.1 introduction

In Chapter III, the effects of the initial texture along the ND on the formation of the HN structure were discussed by employing Cu-Zn alloy plates having sharp textures with <001> or <111> orientations strongly oriented along the ND of the rolling surface. It was found that the specimen with the <001> // ND orientation exhibited a higher strength-ductility balance than that with <111> // ND. Because grains with <001> // ND orientation tended to form more deformation twins in the early stage of rolling, the volume fraction of twin domains in the HN structure increased, and the HN structure developed after heavy cold rolling. In other words, mechanical twinning strongly depends on the crystallographic orientation. However, the crystallographic orientation along the RD should also affect mechanical twinning as well as the orientation along ND. Nevertheless, there have been only a few reports on this topic as far as the authors know.

In this chapter, as an extension of Chapter III, the effects of crystallographic orientation along the RD on deformation twin formation were investigated by employing a specimen with a sharp texture of <001> // ND. In addition, the evolution of the HN structure and the relationship between mechanical properties and rolling reduction were systematically studied.

4.2 Experimental procedure

The specimens used were the Cu-Zn-Sn alloy, as described in Chapters 2 and 3. As mentioned in Section 3.3.1, the cross section of the as-received hot-extruded bar of the alloy has a prominent {001} texture, and the orientation perpendicular to the ND is random (as shown in Fig. 4.1). Twinning behaviors at the early stage of rolling were studied in grains with orientations along the RD parallel to <100>, <210> and <110>. The specimens were unidirectionally rolled to a maximum thickness reduction of 90% at RT.

The experimental conditions for texture measurements, microstructural observations, and tensile tests were the same as those in Chapters II and III.

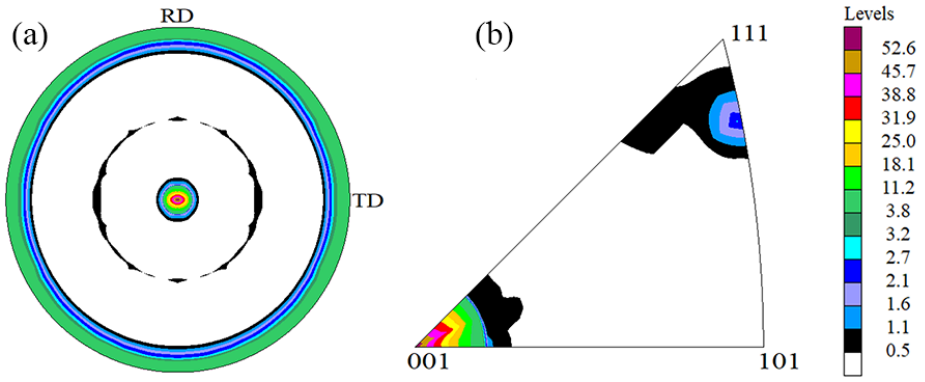

Fig. 4.1 (a) Pole figure and (b) inverse pole figure of ND plane before rolling.

4.3 Result

4.3.1 Mechanical twinning at the early stage of rolling

The texture of the specimen before rolling, as measured by XRD, is shown in Fig. 4.1. It is evident from the pole figure and IPF of the ND plane in Fig. 4.1, that the <001> direction is sharply oriented along the ND (the maximum accumulation intensity is more than 52.6). It was also observed that the orientation perpendicular to the ND was random. More than 100 grains with <100>, <210>, or <110> directions parallel to the RD were chosen for observation to investigate the relationship between RD orientation and mechanical twinning. Grains with orientations that deviated within ±10° from the <100>, <210>, and <110> directions were regarded as having the same orientation. Fig. 4.2 displays the band contrast maps of the specimens with different RD orientations subjected to 15% cold rolling. Grains with RD // <100>, <210> and <110> orientations are indicated by red, yellow and green colors in Figs. 4.2 (a), (c) and (e), respectively. In addition, the twin boundaries (coherent Σ3 grain boundaries) are denoted by red lines in Figs. 4.2 (b), (d), and (f), respectively. It was confirmed that mechanical twinning occurred in all grains of interest, even with different RD orientations. The twin fractions in the specimens after 15% and 20% rolling were investigated, and the results are summarized in Fig. 4.3. After 15% rolling, the twinning frequencies within the grains with the {001}<100> and {001}<210> orientations were almost the same, and the grains with the {001}<110> orientation had the highest value. After 20% rolling, although the twinning frequencies increased compared to 15% rolling, the order of the twinning frequency among the three orientations did not change.

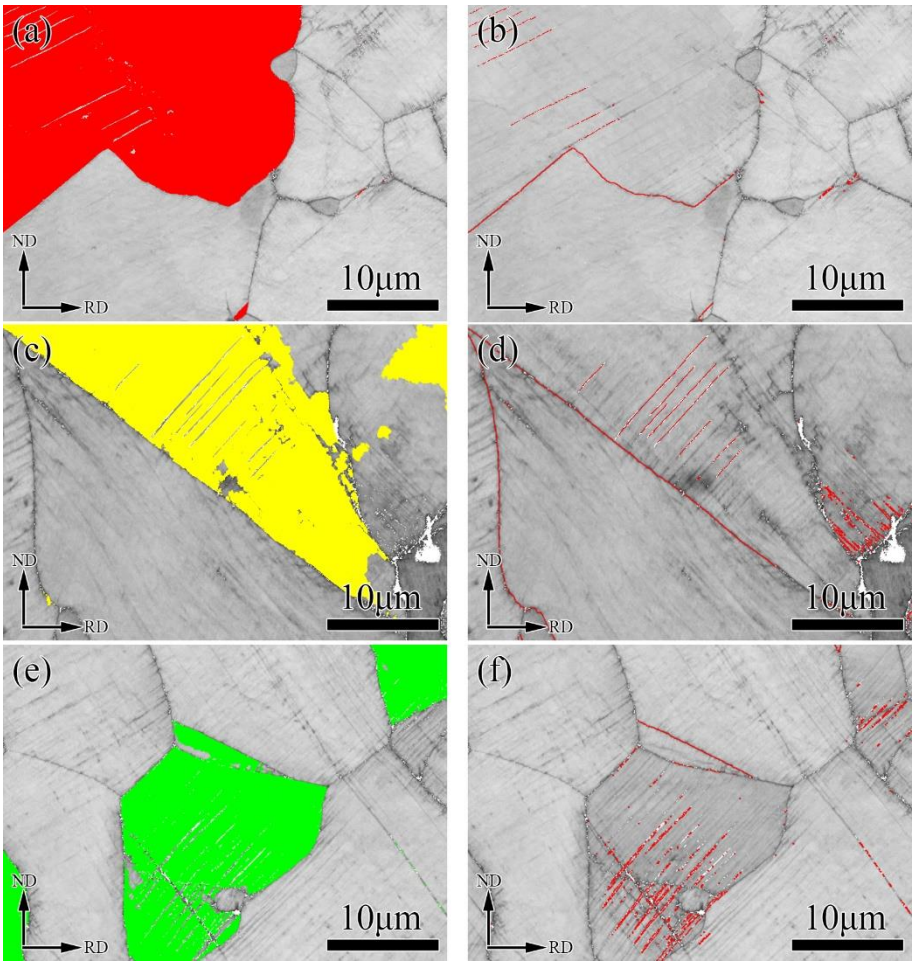

Fig. 4.2 (a) (c) (e) Band contrast maps of a specimen cold-rolled to 15% reduction. The red, yellow, and green colored grains correspond to those with RD parallel to <100>, <210>, and <110>, respectively. (b) (d) (f) Twin (Σ3) boundaries indicated by red lines superimposed on (a), (c) and (e).

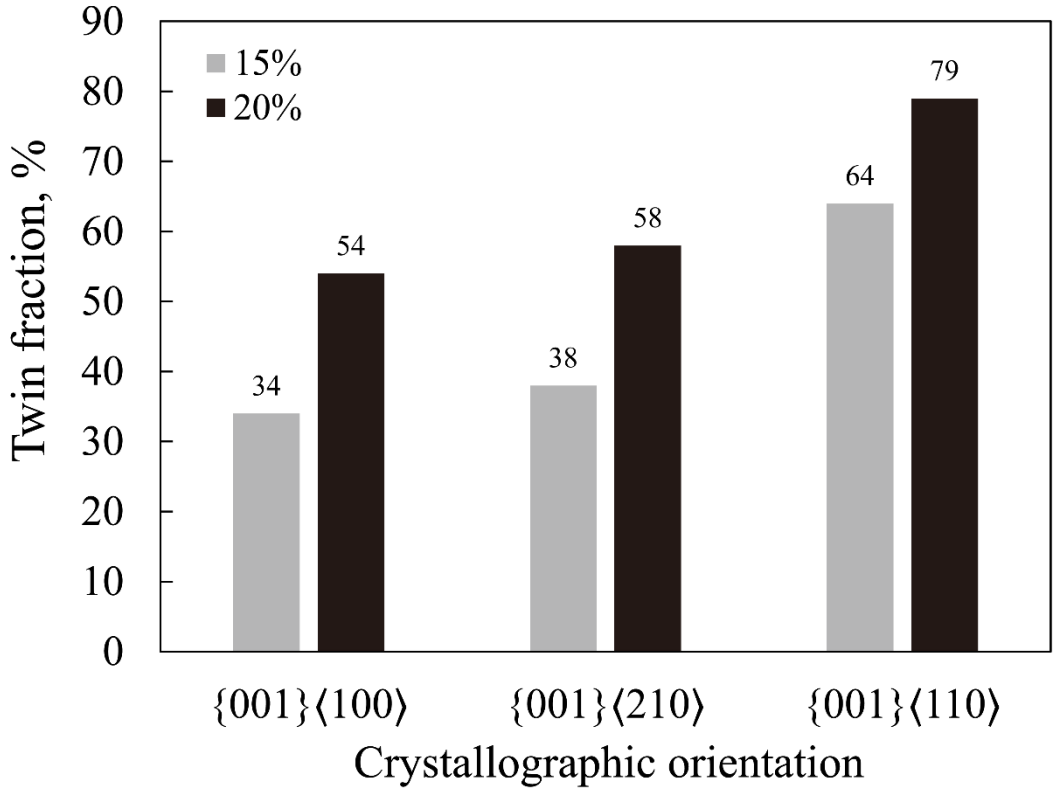

Fig. 4.3 Fractions of twinned grains to whole grains with {001}<100>, {001}<210> and {001}<110> orientations.

4.3.2 Evolution of HN structure

Fig 4.4 shows SEM-BSE images of the specimens before and after 50% rolling. The initial grains before rolling exhibited nearly equiaxed shapes and often contained annealing twins. However, after 50% rolling, the grains elongated along the RD, and mechanical twinning occurred in most of the grains. The average angle between the twin boundaries and RD was approximately 30°. After rolling to 60%, the grains further elongated along the RD, and deformation twins were detected in the entire grains. As shown in Fig. 4.5 (a), the twin-boundary planes rotated geometrically to approach the RD, and the angle from the RD became approximately 20°. In addition, it should be noted that shear bands were formed to subdivide the twinned grains to develop the twin domains. After 70% rolling, as shown in Fig. 4.6, the twin boundaries were almost parallel to the RD. It can also be observed in Fig. 4.6 that the twin boundaries continuously rotate even within the same twin domain surrounded by shear bands. Therefore, it is evident that the shear bands not only subdivide the twinned grains to develop twin domains but also induce crystallographic rotation of the twin-boundary planes nearly parallel to the RD. Some twin domains were further subdivided by shear bands after 80% cold-rolling. Moreover, the evolution of the lamellar structure was first identified at this rolling stage, as indicated by the dashed lines in Fig. 4.7. After 90% rolling, as displayed in Fig. 4.8 (a), the area fraction of the lamellar grains increased compared to that at 80% rolling. The SEM-EBSD analysis revealed that there are two types of deformation twin domains with different crystallographic orientations, as shown in Figs. 4.8 (b) and (c), i.e., ND // <111> and RD // <211>, or ND // <111> and RD // <110>. These characteristic crystallographic orientations of the twin domains are consistent with those reported previously [4.1, 4.2]. However, after 60% rolling, as shown in Figs. 4.5 (b) and (c), the orientation of the twin domains deviated by 24° ± 6° from the above-mentioned orientation. Therefore, the orientation of the domains was continuously and gradually rotated toward the above two characteristic orientations during the heavy cold-rolling process. Analysis of the orientation components in Figs. 4.5 and 4.8 also confirmed the evolution of conventional rolling texture components of the Brass({110}<112>), Goss({110}<001>), and S({123}<634>) orientations. The orientation components are discussed in detail in Section 4.3.3.

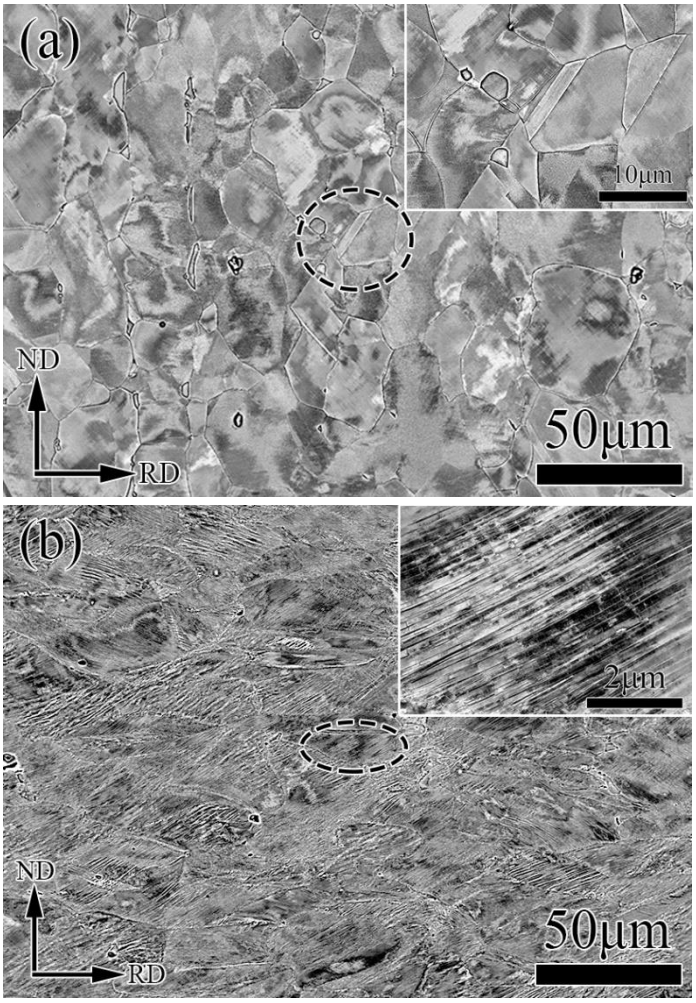

Fig. 4.4 SEM-BSE images of specimen (a) before and (b) after 50% rolling. The inset in each figure shows an enlarged image of the portion indicated by the dashed line.

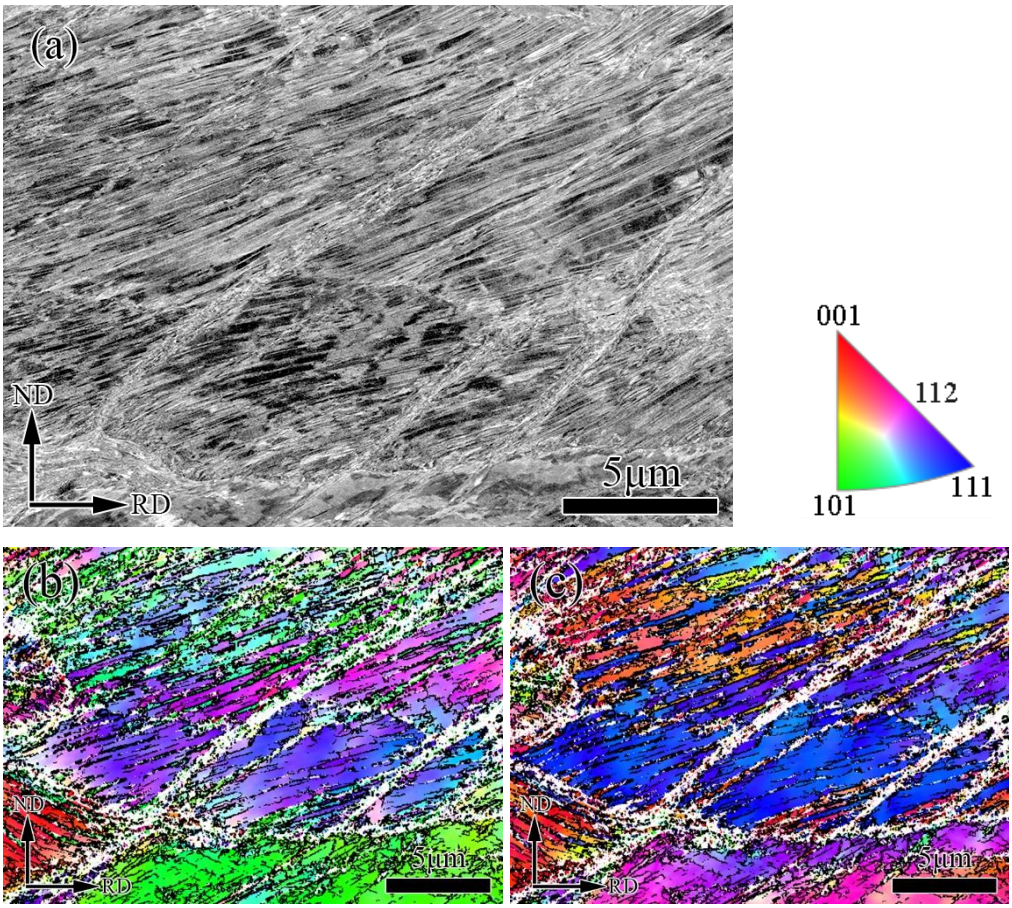

Fig. 4.5 (a) SEM-BSE image of a specimen cold-rolled to 60% reduction. (b) and (c) Inverse pole figure maps taken in the same area as in (a). Color decoding is parallel to (b) ND and (c) RD.

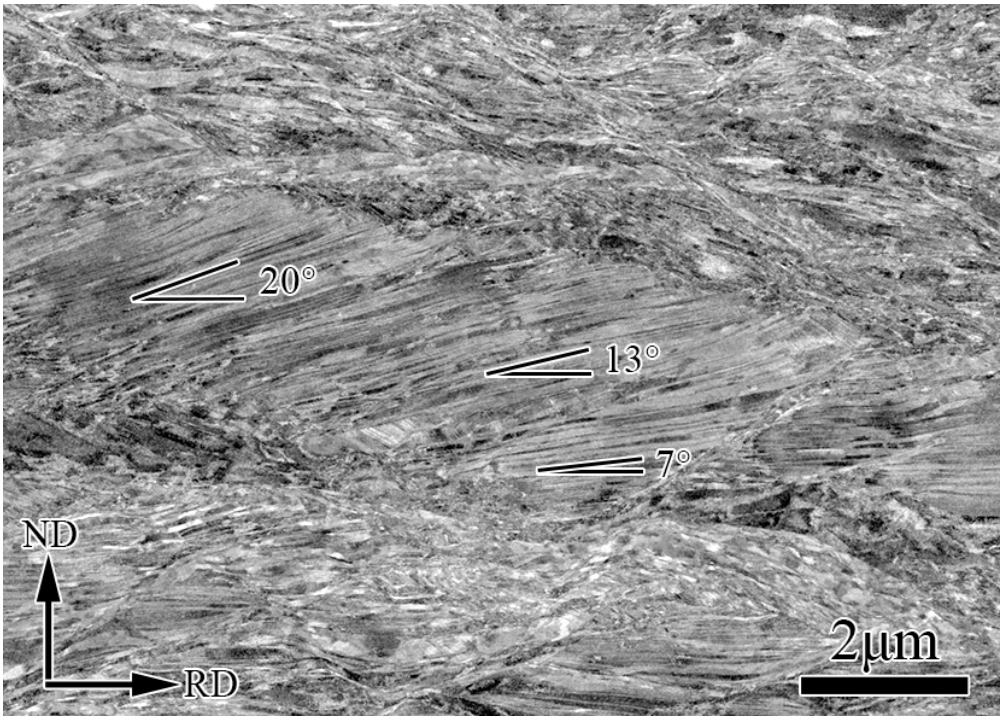

Fig. 4.6 SEM-BSE image of the specimen cold-rolled to 70% reduction, showing twin boundaries continuously rotated within a twin domain.

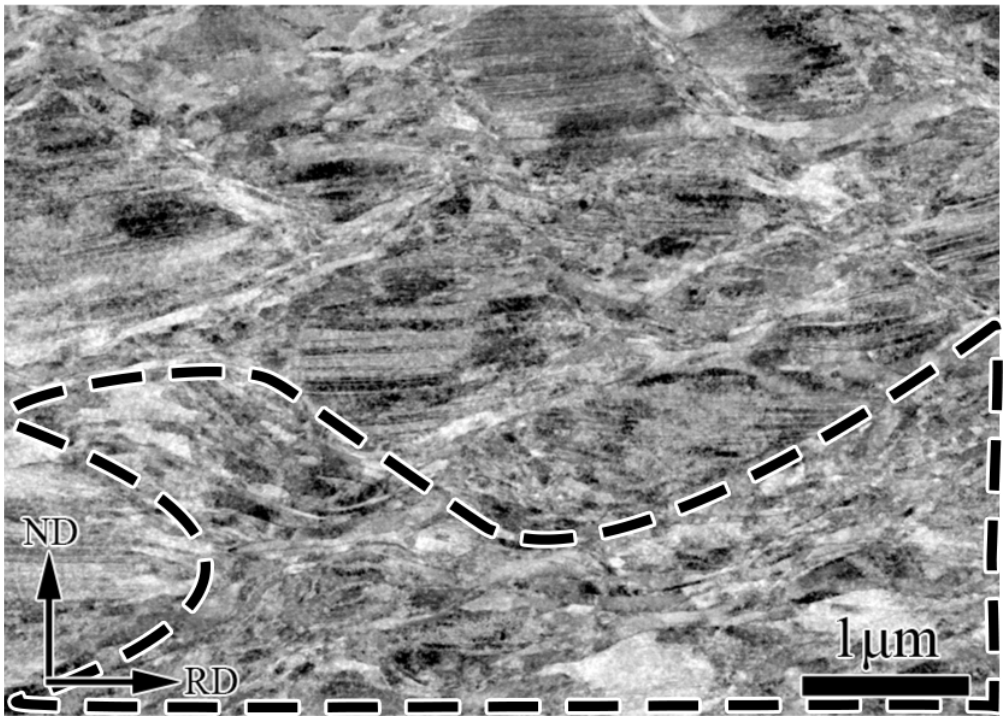

Fig. 4.7 SEM-BSE image of the specimen cold-rolled to 80% reduction.

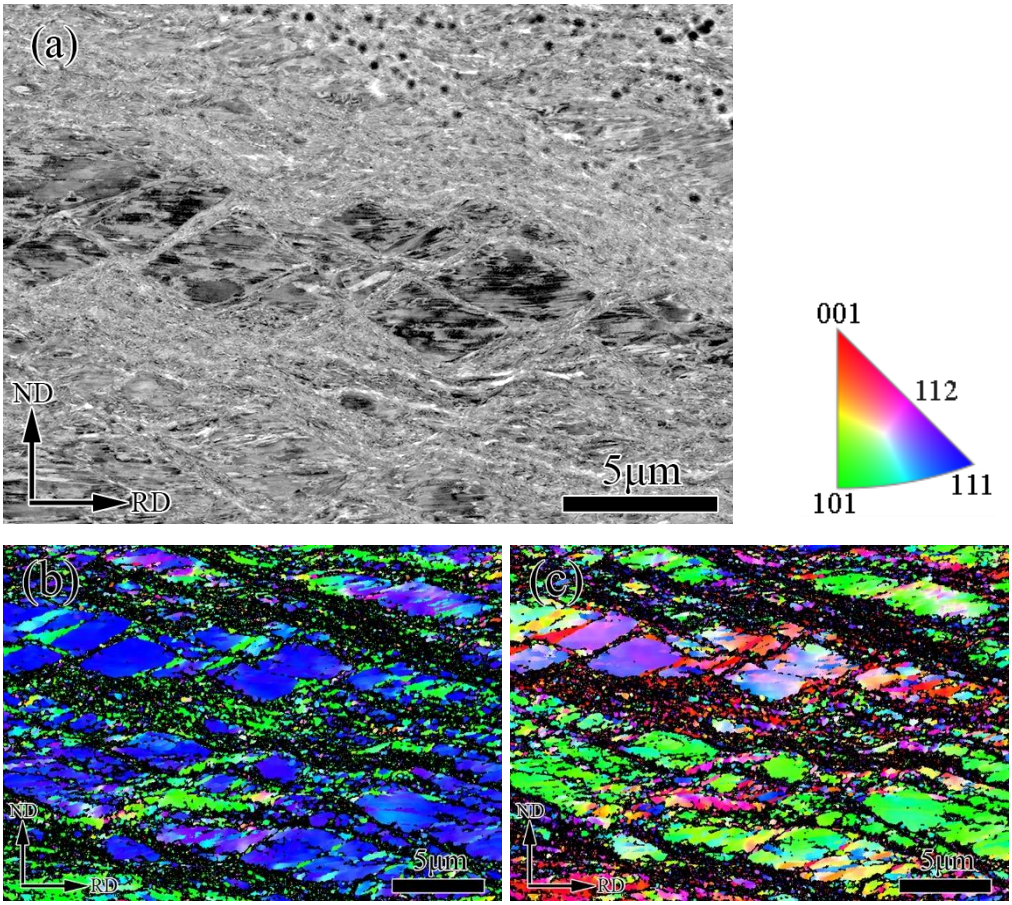

Fig. 4.8 (a) SEM-BSE image of a specimen cold-rolled to 90% reduction. (b) and (c) Inverse pole figure maps taken in the same area as in (a). Color decoding is parallel to (b) ND and (c) RD.

4.3.3 Variation in volume fractions of texture components

SEM-EBSD observations revealed that twin domains with the characteristic orientations of {111}<211> and {111}<110> were formed at 70% rolling. The Brass, Goss and S orientations were also detected. The variations in the texture components developed in the specimens cold-rolled from 70% to 90% were investigated. The volume fractions of the above-mentioned texture components were obtained from the RPFs and ODFs. The results are summarized in Fig. 4.9. The volume fraction of the twin domains decreased with rolling reduction, but in contrast, the volume fractions of the Brass, Goss and S components increased.

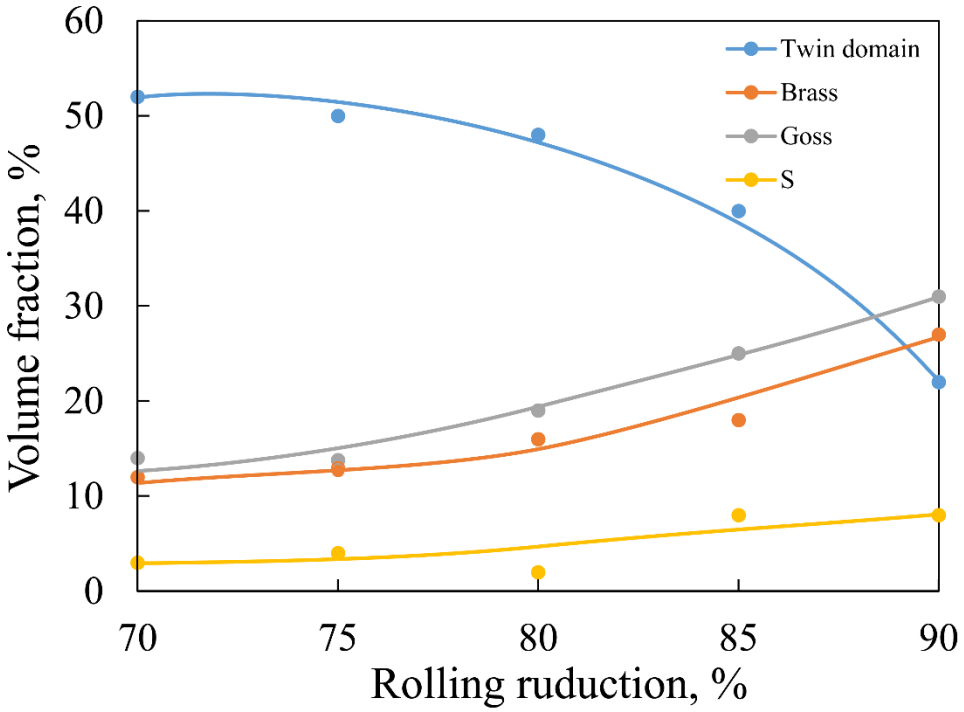

Fig. 4.9 Changes in the volume fraction of major texture components in the specimens during cold rolling from 70% to 90% reduction.

4.3.4 Tensile properties

Fig. 4.10 shows the summarized results of the changes in the tensile strength and fracture strain values of the specimens during cold rolling. Up to 70% reduction, the ductility increased as well as tensile strength with increasing reduction. Considering the microstructural evolution described in Section 4.3.2, the above improvement in the strength/ductility balance should be attributed to the development of the HN structure. On the other hand, further rolling up to 90% resulted in the loss of strength/ductility balance; a slight increase in strength of approximately 50 MPa and a significant decrease in ductility to approximately half (15% to 8%).

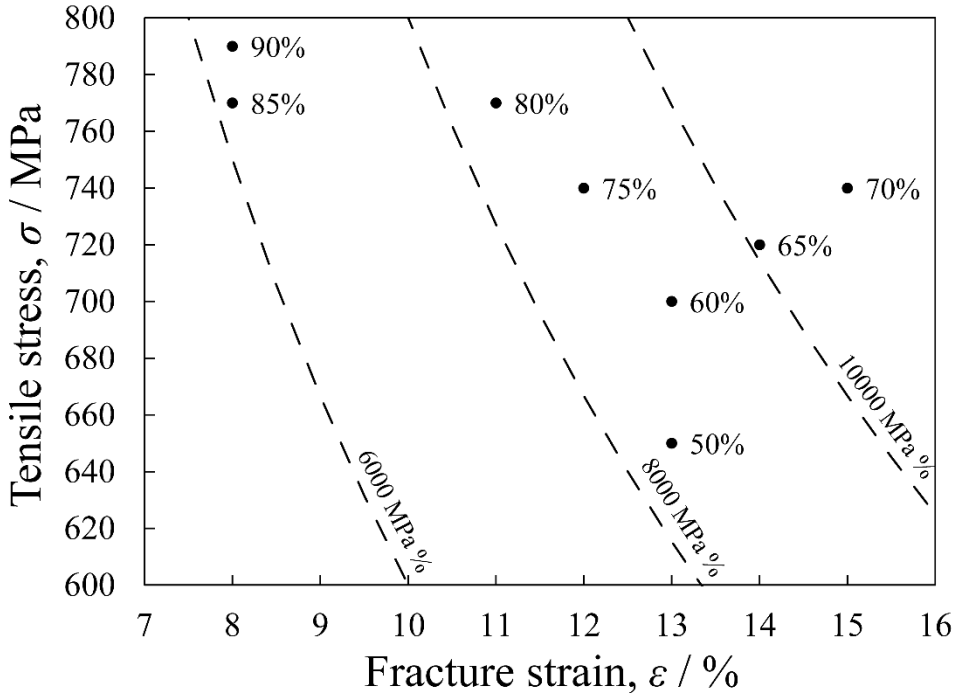

Fig. 4.10 Relationship between tensile stress and fracture strain of specimens cold-rolled to thickness reduction ranging from 50 to 90%.

4.4 Discussion

4.4.1 Rolling direction dependence of mechanical twinning at the early stage of rolling

McCabe *et al.* investigated the orientation dependence of mechanical twinning by a plane strain compression to simulate a rolling process [4.3]. According to the twinning model proposed by McCabe *et al*., the relative difficulty of mechanical twinning is determined by the angle ($\theta\tau$) between the maximum resolved shear stress direction and Burgers vector of the leading partial dislocation. They argued that the threshold stress for mechanical twinning decreases with decreasing $\theta\tau$ [4.3], suggesting that a smaller value of $\theta\tau$ promotes mechanical twinning. The $\theta\tau$ values of the three grain orientations of {001}<100>, {001}<210>, and {001}<110> were evaluated to be 60°, 30°, and 0°, respectively. Thus, {001}<110> is the orientation in which deformation twins are most likely to be introduced, and this estimation agrees well with microstructural observations (Fig. 4.3). On the other hand, the frequency of twinned grains is almost the same between grains with {001}<100> and {001}<210> orientations, although their $\theta\tau$ values are appreciably different. Therefore, the difficulty of mechanical twinning cannot be properly explained by the twinning model proposed by McCabe *et al*. Further research is required to clarify the RD orientation dependence of the mechanical twinning observed in the present study.

4.4.2 Change in the orientation of twin domains

The deformation twin domains after 90% rolling had characteristic crystallographic orientations of {111}<211> or {111}<110>, which agrees well with previous reports [4.1, 4.2]. However, the orientation of the twin domains in the intermediate rolling stage of 60% deviated by approximately 24° from the characteristic orientations. The orientation changes of the twin domains during rolling from 60% to 90% were investigated using SEM-EBSD. Fig. 11 (a) shows the change in the average orientation of the twin domains, which finally achieved the {111}<110> orientation. The twin domains with nearly $(122)[\bar{2}01]$ orientation at 60% rolling reduction gradually rotated the left-handed thread by approximately 30 degrees along the $[01\bar{1}]$ direction and finally transitioned to the $(111)[\bar{1}01]$ orientation. In the same way, the twin region with $(112)[\bar{1}\bar{1}1]$ orientation at 60% rolling reduction also rotated the left-handed thread about 20 degrees along the $[\bar{2}11]$ direction and, then, approached the {111}<211> orientation (Fig. 4.11 (b)). In this way, the various crystallographic orientations of the twin domains, depending on the initial orientations of their mother grains, converge to the characteristic orientation of either {111}<110> or {111}<211> after heavy cold rolling.

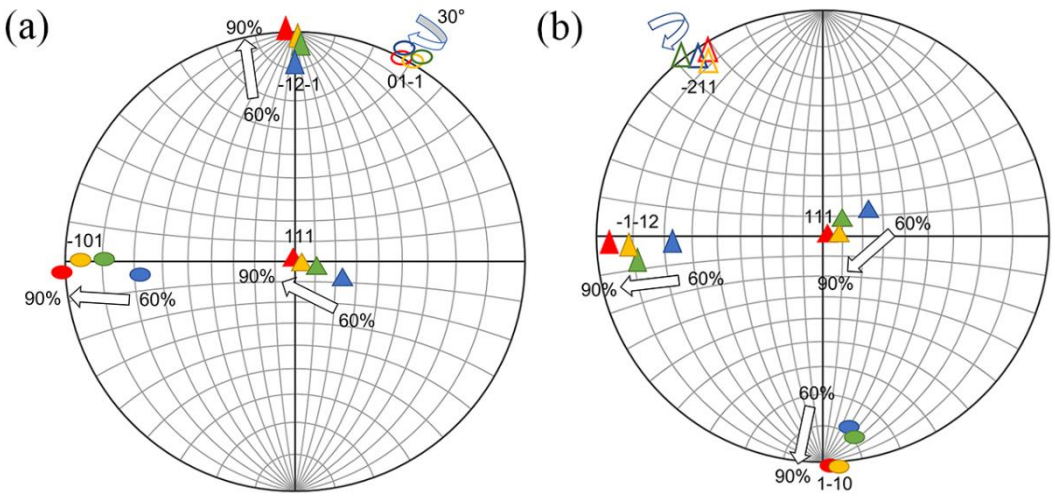

Fig. 4.11 (a) {111}<110> and (b) {111}<211> orientation evolution of deformation twin domains during cold rolling from a 60 to 90% reduction.

4.4.3 Effects of HN structure on mechanical properties

Aoyagi *et al.* conducted a crystal plasticity simulation of the mechanical properties of HN-structured metallic materials and demonstrated that the tensile strength increased with increasing volume fraction of deformation twin domains [4.4]. However, their simulation was based on the assumption that the lamellar boundary and twin boundary spacings were constant. As mentioned in Sections 4.3.3 and 4.3.4, although the volume fraction of the twin domains decreased with increasing rolling reduction in the rolling stage over 70% (Fig. 4.9), the tensile strength increased (Fig. 4.10). Consequently, it is necessary to consider other microstructural factors that affect the mechanical properties of HN-structured metallic materials in addition to the volume fraction of the twin domains. The average lamellar boundary interval in the specimens after 70% and 90% rolling were 306 ± 35 and 126 ± 28 nm, respectively, and the average interspacing of the twin boundaries were 77 ± 26 nm and 48 ± 3 nm, respectively. It is well known that strength increases with decreasing grain size according to the Hall-Petch relationship [4.5, 4.6]. Furthermore, the change in dislocation density after 70% and 90% rolling was estimated using XRD analysis and the modified Williamson-Hall method [4.7] to be 3.61×10^{15} and 4.51×10^{15} m^{-2}, respectively. It is evident that the strengthening at a higher stage of rolling over a 70% reduction is also affected by the increase in the dislocation density. Therefore, the strengthening mechanisms due to the above factors can be condensed as follows: the effects of the decrease in the boundary spacings and the increase in dislocation density exceeded the effects of the decrease in the volume fraction of twin domains to cause strengthening.

Miura *et al.* demonstrated that the presence of twin domains in the HN structure prevented the development of a sharp rolling texture to induce a moderate decrease in ductility [4.8-4.10]. As shown in Fig. 4.8, the volume fraction of the twin domains decreased during rolling from 70% to 90%, and the conventional rolling texture components (Brass, Goss, S orientation) increased. Therefore, the sharp rolling texture became more pronounced with increasing reduction at a higher rolling stage of over 70%, leading to a decrease in ductility. Nevertheless, the influences of other component structures consisting of the HN structure (i.e., shear bands and lamellar grains) on ductility have not been clarified. Therefore, further investigations are necessary.

4.5 Conclusions

A Cu-37.75mass%Zn-0.11mass%Sn alloy specimen with a sharp texture, in which the <001> direction was strongly accumulated along the normal direction of the rolled surface, was subjected to heavy cold rolling. Orientation-dependent mechanical twinning in the rolling direction was investigated. The evolution of the heterogeneous-nano (HN) structure and its effects on the mechanical properties of the specimens were also studied. The main results are summarized as follows.

(1) Mechanical twinning occurred more frequently in grains with the <110> direction close to the rolling direction (RD) during the early stages of rolling.

(2) As the rolling reduction increased at medium stage of rolling, shear bands were introduced and subdivided the twinned grains to develop "eye-shaped" domains. Simultaneously, the twin-boundary planes rotated geometrically to get closer to the RD. After heavy cold rolling, the deformation twin domains possessed characteristic crystallographic orientations of {111}<110> and {111}<211>.

(3) By the rolling reduction from 50% to 70%, the tensile strength and fracture strain increased. The improvement in the strength/ductility balance was attributed to the development of the HN structure. After further rolling to a 90% reduction, a conventional trade-off relationship between strength and ductility appeared.

Reference

[4.1] C. Watanabe, S. Kobayashi, Y. Aoyagi, Y. Todaka, M. Kobayashi, N. Sugiura, N. Yoshinaga and H. Miura: ISIJ Int., 2020, 60(3), 582-589.

[4.2] Y. Li, N. Koga, C. Watanabe, and H. Miura: Mater. Trans., 2022, 63(4), 497-501.

[4.3] R.J. McCabe, I.J. Beyerlein, J.S. Carpenter and N.A. Mara: Nat. Commun., 2014, 5(1), 3806.

[4.4] Y. Aoyagi, C. Watanabe, M. Kobayashi, Y. Todaka and H. Miura: Tetsu-to-Hagane, 2019, 105(2), 140-149.

[4.5] E. O. Hall: Proc. Phys. Soc. Sect. B, 1951, 64, 747-753.

[4.6] N.J. Petch: J. Iron Steel Inst., 1953, 174, 25-28.

[4.7] T. Ungár, and A. Borbély: Appl. Phys. Lett., 1996, 69(21), 3173-3175.

[4.8] H. Miura, M. Kobayashi, Y. Todaka, C. Watanabe, Y. Aoyagi: J. Japan Inst. Metals, 2017, 81(12), 536-541.

[4.9] H. Miura, M. Kobayashi, Y. Todaka, C. Watanabe, Y. Aoyagi, N. Sugiura and N. Yoshinaga: Scr. Mater., 2017, 133, 33-36.

[4.10] H. Miura, Y. Iwama and M. Kobayashi: Mater. Trans., 2019, 60(7), 1111-1115.

Chapter V Summaries and prospects

Previous studies have demonstrated that the introduction of the so-called heterogeneous-nano (HN) structure can significantly enhance the strength of FCC materials with low SFE. In particular, the volume fraction of the twin domains in the HN structure plays an important role in improving strength. Research on the evolution of the HN structure indicated that the twin domains in the HN structure developed from twinned coarse grains. Therefore, mechanical twinning occurring during the early stage of rolling should significantly affect the volume fraction of twin domains that eventually develop. Based on previous studies, the effects of the cold rolling process and crystallographic orientation on mechanical twinning in the early stage of rolling and the development of the HN structure were systematically investigated.

In Chapter II, different cold-rolling processes were applied to rectangular Cu-37.75Zn-0.11Sn (mass%) alloy specimens. One was conventional unidirectional rolling up to a 90% reduction in thickness, and the other was rotational rolling, in which the rolled surface rotated 90° around the rolling direction during the early stages of cold rolling (0~50%), and subsequently unidirectionally rolled up to a total reduction of 90%. After 50% rolling, the ratio of twinned grains to all grains in the rotationally rolled specimen was larger than that in the unidirectionally rolled specimen. This is because the orientation of the rolled surface changes significantly during rotational rolling. Therefore, mechanical twinning should occur even in grains with orientations that make it difficult to form deformation twins during unidirectional rolling, by varying the rolling plane during rotational rolling. In other words, the orientation of the normal plane strongly affects the mechanical twinning in the early stage of rolling. Owing to the increase in deformation twins at the early stage of rolling, after 90% rolling, the rotationally rolled specimen exhibited a finer size and larger volume fraction of deformation twin domains than the unidirectionally rolled specimen. A larger volume fraction of twin domains in rotationally rolled specimens leads to higher strength than that in unidirectionally rolled specimens. Hence, rotational rolling significantly affects the formation of the HN structure, as well as the mechanical properties. Improvements in the fabrication processes based on the crystallographic orientation can be developed as a new method for controlling the HN structure.

The experimental results presented in Chapter II strongly suggest that the initial texture of the normal plane is essential for mechanical twinning during the early stage of cold rolling. The effects of the initial orientation in the normal direction on the evolution of the HN structure are discussed in Chapter III. Two specimens with <001> or <111> texture parallel to the plane normal to the specimen (referred to as <001> or <111> specimen) were prepared from a Cu-37.75Zn-0.11Sn (mass%) alloy bar. The difficulty of mechanical twinning in a grain can be determined by the ratio of the maximum Schmid factor for twinning partial (m_T) to the maximum Schmid factor for perfect dislocation (m_S). The frequency of mechanical twinning at the early stage of rolling was higher in the <001> specimens, which had a relatively higher volume fraction of <001> oriented grains with larger m_T/m_S. Therefore, it can be reasonably understood that more deformation

twins could be introduced in the <001> specimen to evolve a higher volume fraction of twin domains in the HN structure than that in the <111> specimen. This resulted in the strength of the <001> specimen being higher than that of the <111> specimen. In addition, the evolution of texture in the ND plane during rolling was measured using XRD. Although the final textures of the two specimens were almost identical, their evolutionary processes were clearly different. Notably, the differences in the variation trends of the ND // <111> orientation components were associated with the twin domain. Considering the influence of twin domains on strength, it is strongly suggested that an appropriate rolling reduction exists depending on the initial texture to optimize the mechanical properties. The improvement in the manufacturing process based on the knowledge obtained in this chapter is expected to enhance the mechanical properties of HN-structured materials.

The influence of ND orientation on mechanical twinning was confirmed in Chapter III. However, the crystallographic orientation parallel to the RD also affects twinning, as well as the orientation along the ND. In Chapter IV, the effects of crystallographic orientation in the RD on mechanical twinning at the early stage of rolling were studied using a <001> specimen (as mentioned in Chapter III). The relative difficulty of mechanical twinning is determined by the angle ($\theta\tau$) between the maximum resolved shear stress direction and Burgers vector of the leading partial dislocation. The threshold stress for mechanical twinning decreases with a decrease in $\theta\tau$, suggesting that a smaller value of $\theta\tau$ promotes mechanical twinning. The $\theta\tau$ values for the three grain orientations({001}<100>, {001}<210>, and {001}<110>) were evaluated as 60°, 30°, and 0°, respectively. Thus, {001}<110> is the orientation in which deformation twins are most likely to be introduced, and this estimation agrees well with microstructural observations. In addition, the evolution of the orientation of the twin domains during rolling from 60% to 90% was investigated using SEM-EBSD. The twin domains with nearly $(122)[\bar{2}01]$ orientation at 60% rolling reduction gradually rotated the left-handed thread by approximately 30° along the $[01\bar{1}]$ direction and finally transitioned to the $(111)[\bar{1}01]$ orientation. Similarly, the twin region with the $(112)[\overline{11}1]$ orientation at 60% rolling reduction also rotated the left-handed thread by approximately 20° along the $[\bar{2}11]$ direction and then, approached the {111}<211> orientation. Furthermore, the best strength-ductility balance was achieved after 70% rolling. Considering the microstructural evolution, this improvement could be attributed to the development of the HN structure. Further rolling up to 90% resulted in a slight increase in strength and a significant decrease in ductility, i.e., a decrease in the strength-ductility balance. This result is accompanied by a decrease in the volume fraction of the twin domain. On the one hand, according to Hall-Petch relationship, decreasing in interspacing of the twin and lamellar boundaries leads to an increase in strength. Furthermore, the increase in dislocation density was confirmed using XRD analysis and the modified Williamson-Hall method. In other words, the effects of a decrease in the boundary spacing and an increase in the dislocation density exceeded the effects of a decrease in the volume fraction of the twin domains, causing strengthening. However, the volume fraction of the twin domains decreased, and the conventional rolling texture components increased. Therefore, a sharp rolling texture results in a reduced

ductility.

According to the conclusions in Chapters III and IV, the initial texture significantly influences the evolution of the HN structure after heavy cold rolling and its mechanical properties. The impact of the initial texture on the development of the HN structure is not confined to increasing the volume fraction of twin domains. Recent research has indicated that the orientation of twin domains can be controlled by adjusting the initial texture, allowing one of the two orientations ({111}<110> or {111}<211>) to dominate. Two specimens with {111}<110> or {111}<211> initial textures (referred to as the <110> or <211> specimen) were prepared from the Cu-37.75Zn-0.11Sn (mass%) alloy bar. During the rolling process, although the total volume fractions of the two types of twin domains were almost the same, the {111}<110> oriented twin domains were consistently dominant in the <110> specimen, whereas the volume fraction of the {111}<211> oriented twin domains was higher in the <211> specimen. Additionally, the results of the tensile tests during 50%-90% rolling indicate that the strength-ductility balance of the <211> specimen is superior to that of the <110> specimen. Therefore, the higher strength-ductility balance of the <211> specimen is considered to be associated with a higher volume fraction of twin domains with the {111}<211> orientation. This result is qualitatively consistent with the crystal plasticity simulation of the HN-structured metallic materials. Subsequent studies should clarify the details of texture evolution and the effects of the crystallographic orientation of the twin domains on strength.

In summary, many new and essential findings have been obtained for controlling the HN structure through process improvement and initial-texture control. Although this study used only a copper alloy system, the results and conclusions obtained are believed to be applicable to other FCC HN-structured metallic materials.

Acknowledgments

I would like to express my sincere gratitude to my supervisor, Professor Chihiro Watanabe, for his invaluable guidance, encouragement, and support throughout my dissertation. He always gave me constructive feedback and insightful suggestions, which helped improve the quality and confidence of my presentations. I also greatly benefited from his extensive knowledge and experience.

I am also grateful to collaborative supervisors, Professor Hiromi Miura, Associate Professor Norimitsu Koga and Associate Professor Takahiro Kunimine, for their valuable comments and suggestions on my dissertation. With the assistance of Professor Chihiro Watanabe, Hiromi Miura, and Associate Professor Norimitsu Koga, we have successfully published three articles. One of the articles, entitled "*Microstructures and Mechanical Properties of Cu-38mass%Zn Alloy Fabricated by Different Rolling Pass Schedules*" received a paper award from the Japan Institute of Copper. I would like to thank my thesis advisors, Professor Kazuhiro Ishikawa and Tomotsugu Shimokawa, for their invaluable guidance on my dissertation. Additionally, thanks to my advisor, Associate Professor Yoji Miyajima, for his guidance and support in both my academic and social lives.

I would like to thank my coursemates and friends at the Materials Engineering Laboratory and Mr. Yuki Imozuka and Yoshihiro Matsuura for their help and support during my study. They shared their skills and resources with me and offered me technical assistance whenever I needed them. Mr. Hua Jiang, Hailun Zhou, and Hao Wu helped me in my research and also made my study life more enjoyable and memorable.

Finally, I would like to express my deepest gratitude to my parents for their unconditional love and support. Throughout my 6 years of studying abroad, they always believed in me and gave me the best.